Myeloid-derived miR-223 regulates intestinal inflammation via repression of the NLRP3 inflammasome

Viola Neudecker,[1,14] Moritz Haneklaus,[2] Owen Jensen,[13,14] Ludmila Khailova,[14] Joanne C. Masterson,[3,13] Hazel Tye,[4,5] Kathryn Biette,[3,13] Paul Jedlicka,[10] Kelley S. Brodsky,[14] Mark E. Gerich,[11,13] Matthias Mack,[6] Avril A.B. Robertson,[7] Matthew A. Cooper,[7] Glenn T. Furuta,[3,13] Charles A. Dinarello,[9,12] Luke A. O'Neill,[2] Holger K. Eltzschig,[8,14] Seth L. Masters,[4,5]* and Eóin N. McNamee[13,14]*

[1]Clinic for Anesthesiology, University Hospital of Ludwig-Maximilians-University, 80539 Munich, Germany
[2]School of Biochemistry and Immunology, Trinity Biomedical Sciences Institute, Trinity College Dublin, Dublin 2, Ireland
[3]Gastrointestinal Eosinophilic Disease Program, Section of Pediatric Gastroenterology, Hepatology, and Nutrition, Children's Hospital Colorado, Aurora, CO 80045
[4]Division of Inflammation, The Walter and Eliza Hall Institute of Medical Research, Parkville, VIC 3052, Australia
[5]Department of Medical Biology, The University of Melbourne, Parkville, VIC 3010, Australia
[6]Department of Internal Medicine II, University Hospital Regensburg, 93053 Regensburg, Germany
[7]Institute for Molecular Bioscience, The University of Queensland, Brisbane City, QLD 4067, Australia
[8]Department of Anesthesiology, University of Texas Medical School at Houston, Houston, TX 77030
[9]Department of Medicine, Radboud University Medical Center, 6525 GA Nijmegen, Netherlands
[10]Department of Pathology, [11]Division of Gastroenterology and Hepatology, [12]Department of Medicine, [13]Mucosal Inflammation Program, and [14]Department of Anesthesiology, School of Medicine, University of Colorado, Anschutz Medical Campus, Aurora, CO 80045

MicroRNA (miRNA)-mediated RNA interference regulates many immune processes, but how miRNA circuits orchestrate aberrant intestinal inflammation during inflammatory bowel disease (IBD) is poorly defined. Here, we report that miR-223 limits intestinal inflammation by constraining the nlrp3 inflammasome. miR-223 was increased in intestinal biopsies from patients with active IBD and in preclinical models of intestinal inflammation. *miR-223*$^{-/y}$ mice presented with exacerbated myeloid-driven experimental colitis with heightened clinical, histopathological, and cytokine readouts. Mechanistically, enhanced NLRP3 inflammasome expression with elevated IL-1β was a predominant feature during the initiation of colitis with miR-223 deficiency. Depletion of CCR2^{+} inflammatory monocytes and pharmacologic blockade of IL-1β or NLRP3 abrogated this phenotype. Generation of a novel mouse line, with deletion of the miR-223 binding site in the NLRP3 3′ untranslated region, phenocopied the characteristics of *miR-223*$^{-/y}$ mice. Finally, nanoparticle-mediated overexpression of miR-223 attenuated experimental colitis, NLRP3 levels, and IL-1β release. Collectively, our data reveal a previously unappreciated role for miR-223 in regulating the innate immune response during intestinal inflammation.

INTRODUCTION

Inflammatory bowel diseases (IBDs), namely Crohn's disease (CD) and ulcerative colitis (UC), affect nearly 2 million people in the United States. Their etiologies remain elusive, as they involve complex interactions between genetic, environmental, and immunoregulatory factors. UC is restricted to the colon and is a continuous superficial disease, involving predominantly the colonic mucosa, whereas CD can involve any segment of the gastrointestinal tract, with two-thirds of patients presenting with disease in the immunologically active terminal ileum. For both UC and CD, current hypotheses propose that damage to the intestinal mucosa occurs as a result of a dysregulated innate immune response triggered by microbial antigens (Fiocchi, 1998; Nagler-Anderson, 2001; Brazil et al., 2013). Thus, understanding the regulatory circuits that control aberrant innate immune responses in the intestine is critical to our understanding of IBD pathogenesis.

MicroRNAs (miRNAs) are emerging as critical gene regulators in a host of cellular processes, including inflammation. They are endogenous, noncoding, single-stranded RNAs that are 20–23 nucleotides in length and exert regulatory functions through complementary base pairing to the 3′ untranslated regions (UTRs) of protein-coding mRNAs. Currently, the role of miRNAs in mucosal immunity and IBD pathogenesis remains underexplored. However, recent investigations suggest that distinct miRNAs play a crucial role in the maintenance of immune homeostasis (O'Connell et al., 2010; Eulalio et al., 2012; Hsu et al., 2012). Chief among these, miR-223 is emerging as an important regulator of the innate immune system and the response to bacterial stimula-

*S.L. Masters and E.N. McNamee contributed equally to this paper.

Correspondence to Eóin N. McNamee: eoin.mcnamee@ucdenver.edu

Abbreviations used: ASC, apoptosis-associated speck-like protein containing a CARD; CD, Crohn's disease; DAI, disease activity index; DSS, dextran sodium sulfate; IBD, inflammatory bowel disease; miRNA, microRNA; UC, ulcerative colitis; UTR, untranslated region.

© 2017 Neudecker et al. This article is distributed under the terms of an Attribution–Noncommercial–Share Alike–No Mirror Sites license for the first six months after the publication date (see http://www.rupress.org/terms/). After six months it is available under a Creative Commons License (Attribution–Noncommercial–Share Alike 4.0 International license, as described at https://creativecommons.org/licenses/by-nc-sa/4.0/).

The Rockefeller University Press $30.00
J. Exp. Med. 2017 Vol. 214 No. 6 1737–1752
https://doi.org/10.1084/jem.20160462

The Journal of Experimental Medicine

Downloaded from http://rupress.org/jem/article-pdf/214/6/1737/1757972/jem_20160462.pdf by guest on 15 March 2025

tion (O'Connell et al., 2010; Dorhoi et al., 2013). miR-223 was first identified and characterized in the hematopoietic system and shown to be specifically expressed in the myeloid compartment (Johnnidis et al., 2008). It is induced during myeloid differentiation and regulated by various transcription factors (Johnnidis et al., 2008). Moreover, miR-223 critically fine-tunes myeloid cell activity and plays various roles in inflammatory diseases by regulating multiple gene transcripts including granzyme B, the ubiquitin ligase Roquin, E2F1, NOD-like receptor activation, and the NF-κB pathway(Baek et al., 2008; Li et al., 2010; Pulikkan et al., 2010; Bauernfeind et al., 2012; Haneklaus et al., 2012, 2013). Recent data have revealed up-regulation of miR-223 as a novel biomarker in subsets of patients with IBD (Polytarchou et al., 2015) and in preclinical models of intestinal inflammation (Schaefer et al., 2011; Zhou et al., 2015); nevertheless, there are limited mechanistic studies elucidating how miR-223–regulated gene circuits shape enteric inflammation.

The intracellular NOD-like receptor NLRP3 has emerged as a crucial regulator of intestinal homeostasis. It mediates the assembly of the inflammasome complex in response to microbial ligands, triggering caspase-1 activation and secretion of cytokines IL-1β and IL-18, predominantly from myeloid and epithelial cells. Recent studies suggest that defective NLRP3 inflammasome signaling in the gut contributes to IBD through increased epithelial permeability and detrimental immune responses against invading commensal bacteria (Allen et al., 2010; Zaki et al., 2010). Thus, understanding the molecular regulation of NLRP3 and its dysregulation during aberrant inflammation in IBD is an attractive avenue for therapeutic development. Although NLRP3 has been identified as an miR-223 target in vitro (Haneklaus et al., 2012), the role of miR-223 in the regulation of intestinal NLRP3 during IBD is unknown.

In this study, we identify miR-223 as a critical regulator of the myeloid-specific NLRP3 inflammasome during intestinal inflammation. Mice genetically deficient in miR-223 display markedly exacerbated experimental colitis, as indicated by increased immune infiltration (neutrophils and monocytes), hyperactivated NLRP3, and IL-1β release. Generation of a mouse line with a deletion of the miR-223 binding site in the NLRP3 3′ UTR phenocopies *miR-223*$^{-/y}$ mice, with exacerbated colitis and increased NLRP3 activity. Finally, nanoparticle delivery of miR-223 mimetics attenuates experimental colitis and restores the cytokine balance. Thus, we propose that miR-223 functions as a critical rheostat controlling NLRP3 inflammasome activity and regulates the inflammatory tone of the intestine.

RESULTS

Increased colonic miR-223 expression correlates with active inflammation during IBD and experimental dextran sodium sulfate (DSS)–colitis

During intestinal inflammation such as occurs in IBD, there is a marked influx of various leukocyte populations into the inflamed intestine, which initiates tissue injury. Our understanding of how miRNA circuits regulate this innate immune sequelae is limited. We aimed to identify specific miRNAs that correlate with the inflammatory milieu and that hold promise as novel therapeutic targets. We identified miR-223 as a known myeloid-specific miRNA with significantly higher expression during active inflammation from mucosal biopsies of IBD patients (Fig. 1 A). In addition, whereas expression was negligible in the uninflamed mouse colon, administration of an epithelial irritant, DSS, dramatically induced expression of miR-223 (Fig. 1 B). Of note, this induction precedes histological evidence of inflammation (day 2 after treatment) and is indicative of an early myeloid inflammatory influx (Fig. 1 C). To address whether the induction of miR-223 was a result of induced gene expression from tissue-resident leukocytes compared with infiltrating immune cells, we depleted either neutrophils (anti-Ly6G) or monocytes (anti-CCR2) with antibodies during the onset of DSS treatment. Of note, neutrophil depletion significantly reduced miR-223 expression (35%), but monocyte depletion attenuated miR-223 expression (67%) back to the level of uninflamed controls (Fig. 1 D). Thus, the initial source of miR-223 during acute colitis is from infiltrating neutrophils and monocytes. These data provided the rationale to assess the biological function of miR-223 during experimental colitis.

Exacerbated DSS-colitis in miR-223$^{-/y}$ mice

Based on the previous data showing increased miR-223 in IBD biopsies and preclinical models, we tested the hypothesis that increased miR-223 during active intestinal inflammation plays a functional role by performing a series of DSS-colitis experiments with *miR-223*$^{-/y}$ mice. Although *miR-223*$^{-/y}$ mice did not display any aberrant colonic inflammation at baseline, they exhibited markedly increased disease severity compared with WT counterparts during DSS-colitis as measured by weight loss and disease activity indices (Fig. 1, E and F). *miR-223*$^{-/y}$ mice presented with a significant increase in colonic ulceration and occult bleeding by day 3, at which time WT mice displayed only a mild histological inflammation and no gross ulceration (Fig. 1 G). Finally, enhanced colitis corresponded with a marked increase in all indices of colonic histopathology, including inflammatory infiltrates and overall tissue injury (Fig. 1, G–I).

Recent work has demonstrated that certain mouse strains, in particular *nlrp6*$^{-/-}$ and *IL-18*$^{-/-}$ develop a dysbiotic microbiome and present with a transmissible, context-specific susceptibility to intestinal inflammation compared with cohoused littermates (Elinav et al., 2011; Nowarski et al., 2015). To test whether the exacerbated colitis in *miR-223*$^{-/y}$ was transmissible or mediated by an intrinsic mechanism, we subjected cohoused *miR-223*$^{-/y}$ and WT controls to DSS-colitis. As shown in Fig. S1 (A and B), whereas cohoused *miR-223*$^{-/y}$ mice displayed modestly variable weight loss and disease activity index (DAI) during the course of colitis, there were no significant perturbations observed in the phenotype

Downloaded from http://rupress.org/jem/article-pdf/214/6/1737/1757972/jem_20160462.pdf by guest on 15 March 2025

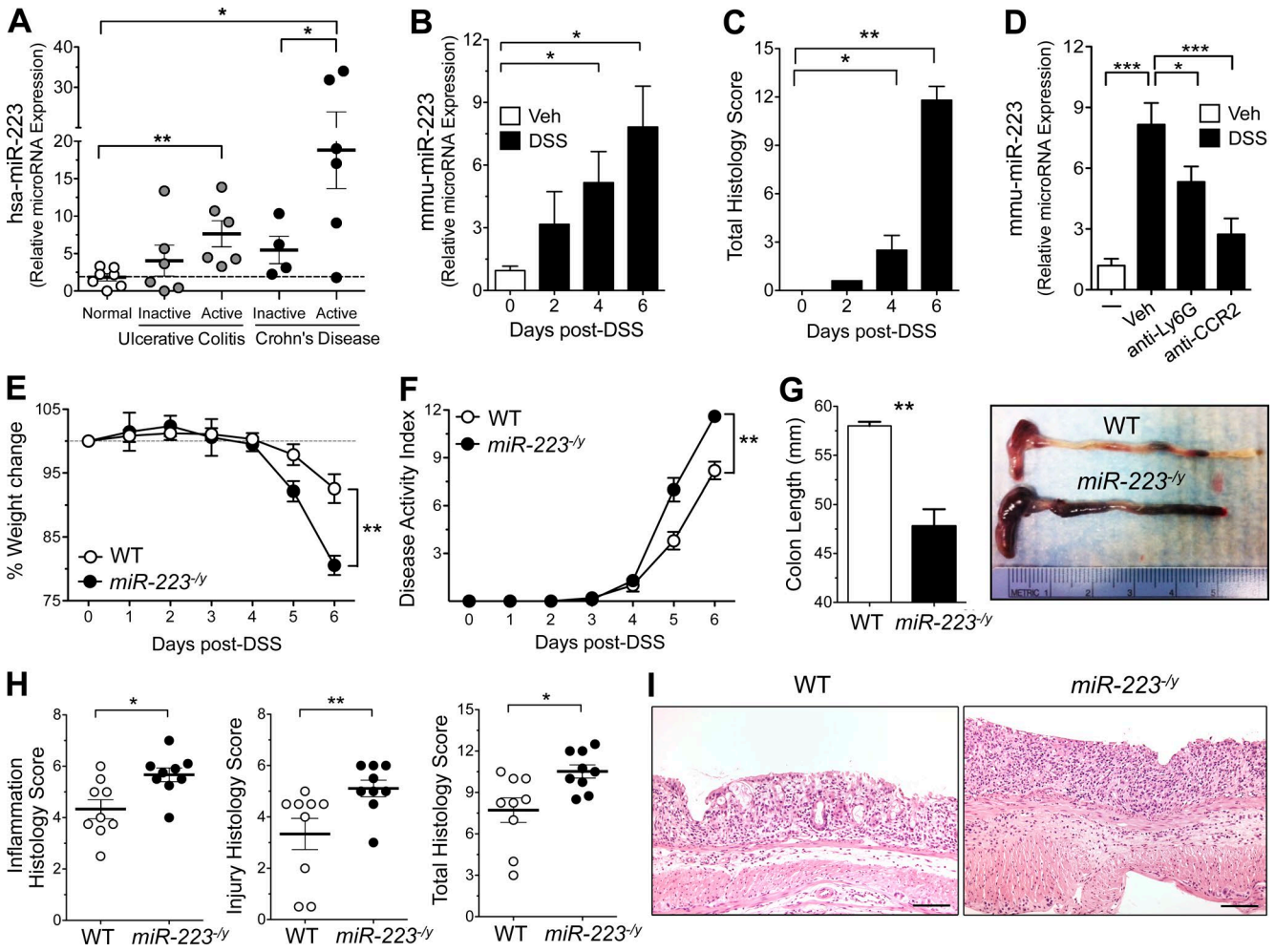

Figure 1. **miR-223 regulates acute intestinal inflammation.** (A) hsa-miR-223 expression was assessed in intestinal mucosal biopsies from patients with either CD or UC. *n* = 4–10 patients/group; statistical significance determined by ANOVA with Bonferroni's multiple comparison test. (B) DSS (3% wt/vol) was administered in drinking water ad libitum to B6.WT mice. Colonic mmu-miR-223 expression was determined from mice undergoing DSS-colitis (days 0, 2, 4, and 6). *n* = 3–5 mice/group; statistical significance determined by ANOVA with Newman–Keuls multiple comparison test. (C) Histopathology scores from DSS-colitis on days 0, 2, 4, and 6 of treatment (3% wt/vol). *n* = 5 mice/group; statistical significance determined by ANOVA with Newman–Keuls multiple comparison test. (D) Neutrophils were depleted with 300 µg (i.p.) anti-Ly6G (1A8) or isotype control on days 0 and 1 after DSS. Monocytes were depleted with 20 µg (i.p.) anti-CCR2 (MC21) or isotype control on days 0 and 1 after DSS. Mice were euthanized on day 2 after DSS, and miR-223 expression was analyzed in colon tissues. *n* = 5 mice/group; statistical significance determined by ANOVA with Newman–Keuls multiple comparison test. (E) Weight loss during DSS-colitis was expressed as the percentage of change from day 0. *n* = 9 mice/group; statistical significance determined by unpaired Student's *t* test. (F) Clinical DAI was a composite of weight change (percentage of day 0), stool score, and occult blood index. *n* = 9 mice/group; statistical significance determined by unpaired Student's *t* test. (G) Colon lengths of DSS-treated mice were assessed at the time of necropsy with representative macroscopic images. *n* = 9 mice/group; statistical significance determined by unpaired Student's *t* test. (H) Histopathology scores from WT and *miR-223*$^{-/y}$ colons after DSS-colitis. *n* = 9 mice/group; statistical significance determined by unpaired Student's *t* test. (I) Representative micrographs of colon H&E from WT and *miR-223*$^{-/y}$ mice 6 d after DSS-colitis. Data are expressed as mean ± SEM; *, $P < 0.05$; **, $P < 0.01$; ***, $P < 0.001$ versus the indicated counterparts from three independent experiments. Bars, 100 µm.

compared with single-housed controls by day 6 after DSS treatment. This was evident by equivalent weight loss, occult bleeding, and diarrhea scores between single and cohoused counterparts. However, cohoused WT mice displayed increased colonic shortening compared with single-housed littermates, indicating a modest effect of cohoused *miR-223*$^{-/y}$ microbiome on some parameters of DSS-colitis (Fig. S1, A and B). Of note, the relative frequency of inflammatory infiltrates into the colon (specifically neutrophils and monocytes) was unchanged between single or cohoused WT and *miR-223*$^{-/y}$ counterparts (unpublished data).

Hematopoietic deficiency of miR-223 enhances susceptibility to DSS-colitis

Although our data depict a significant role for miR-223 in the control of intestinal inflammation, *miR-223*$^{-/y}$ mice, being a

Downloaded from http://rupress.org/jem/article-pdf/214/6/1737/1757972/jem_20160462.pdf by guest on 15 March 2025

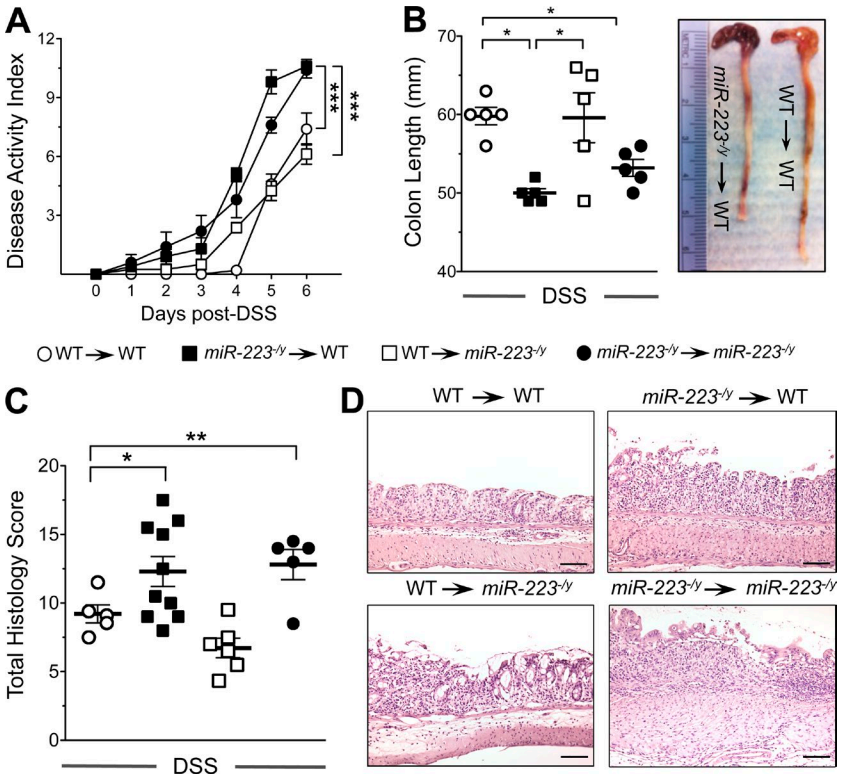

Figure 2. **Hematopoietic-derived miR-223 constrains experimental DSS-colitis.** BM chimeric mice were generated after irradiation of WT (CD45.1) or *miR-223*$^{-/y}$ (CD45.2) mice. 8 wk after irradiation, DSS was administered in drinking water ad libitum (3% wt/vol) for 6 d. (A) Clinical DAI was a composite of weight changes (percentage of day 0), stool score, and occult blood index. n = 5–10 mice/group; statistical significance determined by ANOVA with Newman–Keuls multiple comparison test. (B) Colon lengths were assessed at the time of necropsy, and representative macroscopic images were acquired. n = 5 mice/group; statistical significance determined by ANOVA with Newman–Keuls multiple comparison test. (C) Histopathology scores from WT and *miR-223*$^{-/y}$ colons. n = 5–10 mice/group; statistical significance determined by ANOVA with Newman–Keuls multiple comparison test. (D) Representative micrographs of colon H&E from WT and *miR-223*$^{-/y}$ mice 6 d after DSS-colitis. Data are expressed as mean ± SEM; *, $P < 0.05$; **, $P < 0.01$; ***, $P < 0.001$ versus WT counterpart from two independent experiments. Bars, 100 µm.

whole-body hemizygous knockout strain, do not definitively identify myeloid-derived miR-223 in this phenotype. To address this, we generated BM chimeric animals as previously described (McNamee et al., 2011) to investigate the relative contribution of hematopoietic versus stromal/radio-resistant miR-233 in orchestrating intestinal inflammation. Our data identify hematopoietic-derived miR-223 (*miR-223*$^{-/y}$ → WT recipients) as driving exacerbated colitis, as indicated by increased DAI, weight loss, colon shortening, and histological indices compared with controls (WT → *miR-223*$^{-/y}$ recipients; Fig. 2, A–D). miR-223 has maximal expression in BM-derived egressing neutrophils and monocytes, which are not yet matured within tissues (Johnnidis et al., 2008; Bauernfeind et al., 2012; Haneklaus et al., 2012). Thus, our data suggest that the increase in colonic miR-223 in patients with active IBD and experimental DSS-colitis is derived from infiltrating myeloid cells.

Increased myeloid infiltrate and IL-1β expression in *miR-223*$^{-/y}$ mice during the onset of DSS-colitis

To further dissect the hematopoietic-derived cellular populations driving exacerbated DSS-colitis in *miR-223*$^{-/y}$ mice, we assessed the cellular infiltrate at the early phase of DSS-colitis (day 0–2). Increased histological inflammation and tissue damage in *miR-223*$^{-/y}$ mice was accompanied by an enhanced colonic influx of both neutrophils and monocytes, although tissue macrophage frequencies appeared normal (Fig. 3, A–D). Similar to previous publications, a modest decrease in CD11c^{+} dendritic cells was also observed (Zhou et al., 2015; Fig. 3 E). To further investigate a causative mechanism for exacerbated DSS-colitis in *miR-223*$^{-/y}$ mice, we assessed cytokine expression patterns during early disease (day 2). Surprisingly, an increase in expression of IL-1β compared with WT counterparts was the predominant cytokine phenotype from the colons of *miR-223*$^{-/y}$ mice (Fig. 3 F). Finally, we investigated the expression of neutrophil and monocyte chemokines and demonstrated that the IL-1β–inducible chemokines CXCL1, CXCL2, and CCL2 (Calkins et al., 2002) were significantly induced in *miR-223*$^{-/y}$ colons and correspond with the enhanced influx of both neutrophils and monocytes (Fig. 3. G–I).

Increased NLRP3 inflammasome activity in miR-223$^{-/y}$ mice during DSS-colitis

Based on the finding that myeloid-derived miR-223 regulates intestinal inflammation and that a predominant phenotype of the early colitic response was enhanced IL-1β release, we next investigated a role for the miR-223 target mRNA, NLRP3. The NLRP3 protein was identified as a bona fide miR-223 target (Bauernfeind et al., 2012; Haneklaus et al., 2012; Fig. 4 A) that is conserved across species and has been shown to be critical for intestinal homeostasis and the sensing of bacterial ligands (Zaki et al., 2010, 2011). To define a functional effect of miR-223 deficiency on NLRP3 inflammasome function, we observed an increase in IL-1β protein in colons from *miR-223*$^{-/y}$ mice compared with WT counterparts, both at baseline and after established DSS-colitis (Fig. 4 B). Next we assessed the relative ex-

Downloaded from http://rupress.org/jem/article-pdf/214/6/1737/1757972/jem_20160462.pdf by guest on 15 March 2025

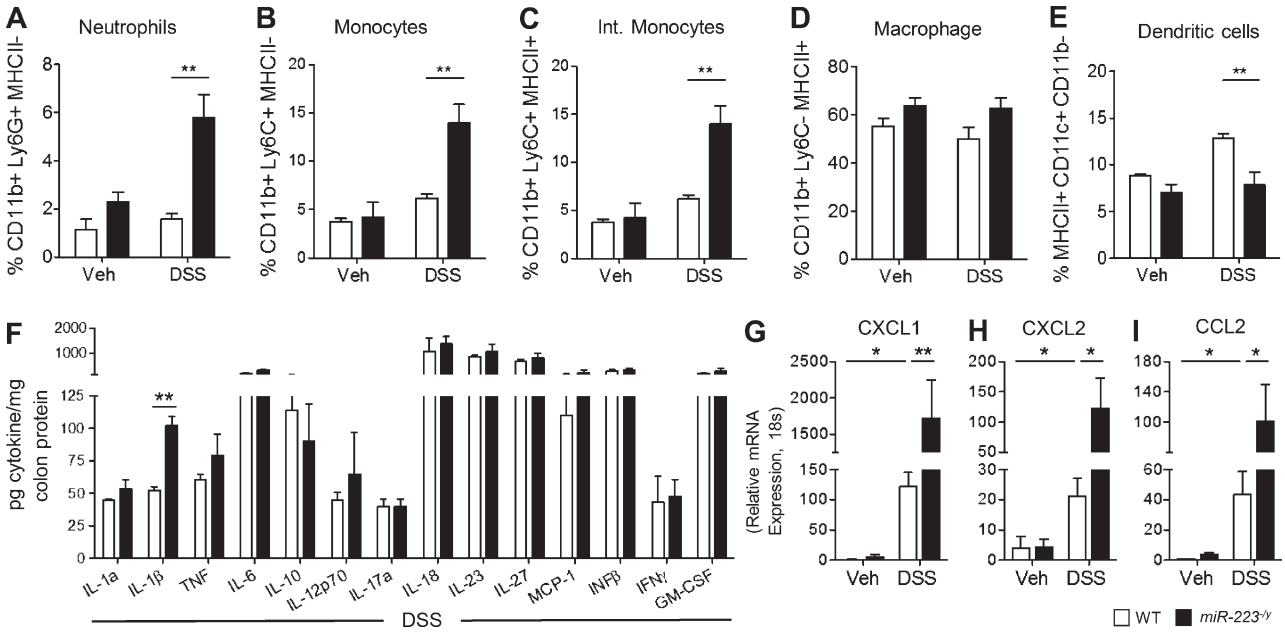

Figure 3. **Onset of colitis in *miR-223*$^{-/y}$ mice is characterized by the enhanced expression of IL-1β and influx of neutrophils and monocytes.** DSS was administered in drinking water ad libitum (3% wt/vol) to WT and *miR-223*$^{-/y}$ mice for 2 d. (A–D) Flow cytometry characterized collagenase digested colons for the presence of live, CD45$^+$ CD11b$^+$ myeloid cells that were neutrophils (Ly6G$^+$ MHCII$^-$; A), monocytes (Ly6C$^+$ MHCII$^-$; B), intermediate monocytes (Ly6C$^+$ MHCII$^+$; C), macrophages (Ly6C$^-$ MHCII$^+$; D), and dendritic cells (MHCII$^+$ CD11c$^+$ CD11b$^-$; E). n = 4 mice/group; statistical significance determined by two-way ANOVA with Bonferroni test. (F) Inflammatory cytokine expression was quantified in whole colon tissues from WT or *miR-223*$^{-/y}$ mice after DSS by LEGENDplex bead array (see Materials and methods) or ELISA (IL-18). n = 4 mice/group; statistical significance determined by unpaired Student's t test. (G–I) Relative gene expression of the neutrophil and monocyte chemokines CXCL1 (G), CXCL2 (H), and CCL2 (I) was measured by RT-PCR from whole colon tissue and expressed relative to 18s. n = 5 mice/group; statistical significance determined by ANOVA with Newman–Keuls multiple comparison test. Data are expressed as mean ± SEM; *, P < 0.05; **, P < 0.01 versus the indicated counterpart from two independent experiments.

pression of NLRP3 protein in whole colonic lysates from mice with DSS-colitis. *miR-223*$^{-/y}$ mice exhibited increased expression of NLRP3 protein (or increased numbers of NLRP3-expressing cells) and secreted IL-1β compared with WT counterparts (Fig. 4 C). Next, we stimulated BMDMs from WT or *miR-223*$^{-/y}$ mice to prime the formation of the inflammasome (LPS treatment) and assessed the secretion of IL-1β protein (after activation with ATP). Activated BMDM from *miR-223*$^{-/y}$ mice exhibited increased expression of NLRP3 protein and mature IL-1β compared with WT cells (Fig. 4 D). Interestingly, although miR-223 deficiency did not affect the mRNA expression of IL-1β, IL-18, or TNF (Fig. 4, E–G), *miR-223*$^{-/y}$ BMDM secreted higher levels of mature IL-1β and IL-18 protein compared with WT cells, without altering TNF (Fig. 4, H–J). These data confirm a selective and functional role for miR-223 in regulating a critical component of myeloid cell activation in the intestine, the NLRP3 inflammasome.

Antibody depletion of CCR2$^+$ inflammatory monocytes dampens IL-1β expression and DSS-colitis in miR-223$^{-/y}$ mice

Based on our observation that monocyte depletion inhibits the expression of miR-223 (Fig. 1 D) and the finding that *miR-223*$^{-/y}$ mice present with increased monocytes and neutrophils during DSS-colitis, we investigated the impact of either monocyte or neutrophil depletion during colitis. Flow cytometry confirmed a selective depletion of either monocytes (anti-CCR2; MC21) or neutrophils (anti-Ly6G, 1A8; Fig. 5, A and B) after treatment. Neutrophil depletion was further confirmed by depletion for iNOS mRNA (Fig. 5 J) but appeared to have no effect on intestinal inflammation. However, anti-CCR2 depletion of inflammatory monocytes abrogated histological indices of colitis and tissue damage (Fig. 5, C and D). Consistent with a previous study (Seo et al., 2015), CCR2$^+$ monocyte depletion further depleted colonic IL-1β levels in *miR-223*$^{-/y}$ mice (Fig. 5 E). We demonstrated that IL-1β mRNA is repressed after CCR2 treatment (Fig. 5 F), as are the transcripts for the IL-1β–induced genes IL-6 and CXCL1. Importantly, expression of TNF mRNA was comparable in both anti-Ly6G and anti-CCR2 groups, indicating a selective role for monocyte-derived IL-1β in driving enhanced colitis pathology in *miR-223*$^{-/y}$ mice (Fig. 5, G–I).

Blockade of the NLRP3 inflammasome or IL-1β abrogates the enhanced pathology of *miR-223*$^{-/y}$ mice during DSS-colitis

Next we investigated whether selective pharmacologic blockade of either the NLRP3 inflammasome or IL-1β would directly further limit colitis in *miR-223*$^{-/y}$ mice.

Downloaded from http://rupress.org/jem/article-pdf/214/6/1737/1757972/jem_20160462.pdf by guest on 15 March 2025

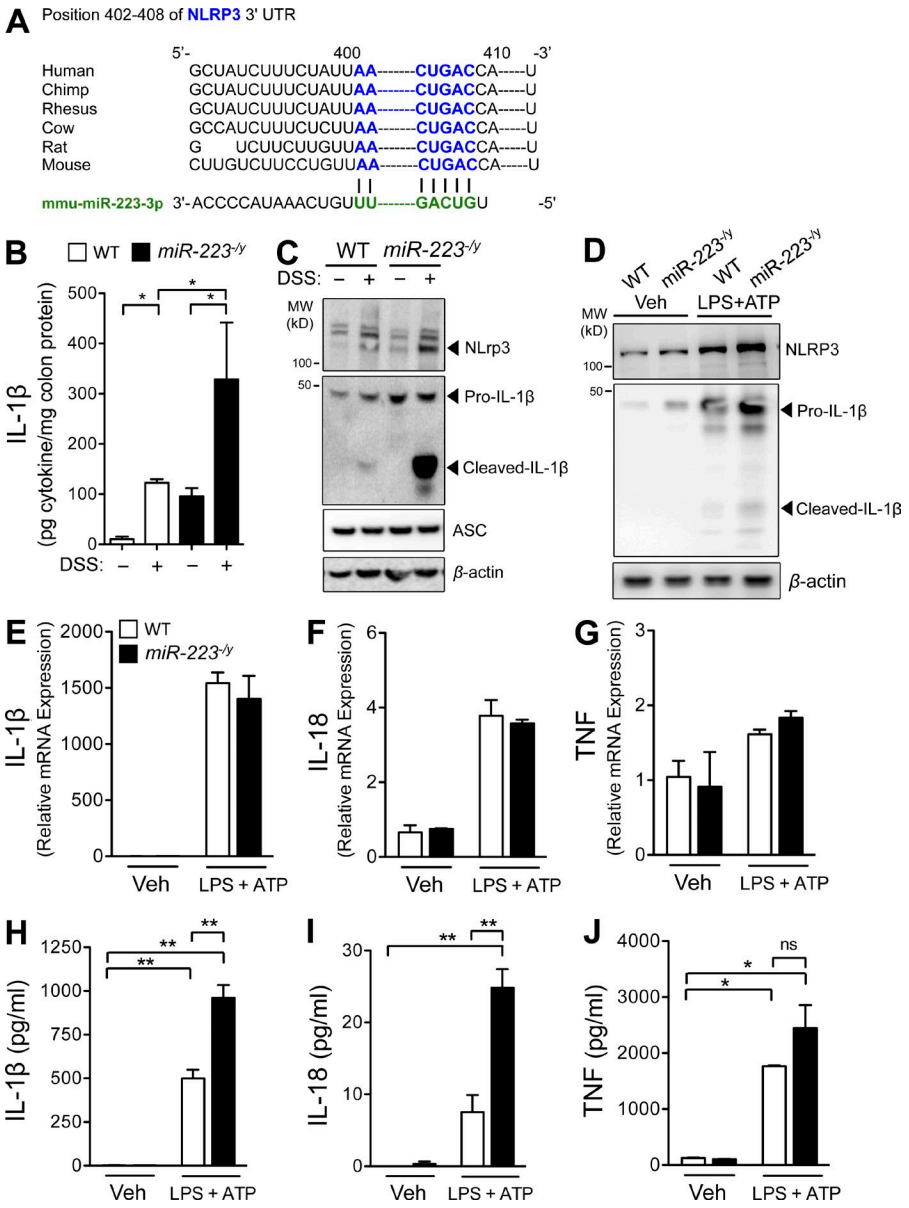

Figure 4. **Increased NLRP3 inflammasome activity in BMDMs and colons from *miR-223*$^{-/y}$ mice during DSS-colitis.** (A) Schematic of in silico miR-223 binding sequence to the 3′ UTR of the mouse NLRP3 and conservation across multiple species. (B) ELISA measurement of IL-1β in whole colon biopsies from WT and *miR-233*$^{-/y}$ mice on day 6 after DSS-colitis. n = 5 mice/group; statistical significance determined by ANOVA with Newman–Keuls multiple comparison test. (C) Western immunoblot assessment of NLRP3, pro–IL-1β, cleaved IL-1β, ASC, and β-actin in whole colon biopsies from WT and *miR-233*$^{-/y}$ mice on day 6 after DSS-colitis. Representative immunoblot from three independent mice. (D) Western immunoblot assessment of NLRP3, IL-1β, and β-actin in BMDM after 6-h treatment with media vehicle or LPS (100 ng/ml). Representative immunoblot from three independent mice. (E–J) BMDMs were cultured for 5 d and primed with LPS (100 ng/ml) for 3 h, and NLRP3 was activated with ATP (1 mM) for 3 h. Gene expression of IL-1β (E), IL-18 (F), and TNF (G) were assessed by quantitative PCR. n = 3–4 mice/group; statistical significance determined by two-way ANOVA with Bonferroni test. Secreted cytokines IL-1β (H), IL-18 (I), and TNF (J), were quantified in cell-free supernatants by ELISA. n = 3–4 mice/group; statistical significance determined by two-way ANOVA with Bonferroni test. Data are expressed as mean ± SEM; *, $P < 0.05$; **, $P < 0.001$ versus the indicated counterpart from two independent experiments.

Therefore, *miR-223*$^{-/y}$ mice were treated with either the NLRP3 inhibitor MCC950 or the IL-1 receptor antagonist anakinra for the duration of DSS-colitis. As shown in Fig. 6, A–D, both treatment regimens significantly attenuated the clinical signs of colitis, including weight loss, DAI, and colon length. Histopathologic indices were further repressed by both MCC950 and anakinra administration (Fig. 6, E and F). We also observed that colonic monocyte and neutrophil frequencies were reduced to those of WT mice treated with DSS (Fig. 6, G and H). Last, although inflammatory cytokines TNF and IL-6 were unaltered, colonic IL-1β was significantly lower after treatment (Fig. 6, I–K). Thus, heightened NLRP3 activation with subsequent increased mature IL-1β accounts for the enhanced experimental colitis in *miR-223*$^{-/y}$ mice.

Generation of miR-223 target site knockout mice (*Nlrp3*^{m223del}) and assessment of NLRP3 function in vitro and in vivo

Our in vitro experiments implicated miR-223 as a critical negative regulator of NLRP3 expression. To test the importance of this interaction in vivo, we generated a mouse with the possibility to conditionally knock out 92 bp of the NLRP3 3′ UTR, including the miR-223 target site, using the CMV-Cre-Lox system. Compared with the available models that interfere with miR-223, namely hemizygous knockout *miR-223*$^{-/y}$ mice (Johnnidis et al., 2008) or mice transplanted with BM expressing an miR-223 "sponge" (Gentner et al., 2009), our approach does not alter the ability of miR-223 to regulate all other targets. There is the possibility that this deletion in the NLRP3 3′ UTR affects folding of the region,

Downloaded from http://rupress.org/jem/article-pdf/214/6/1737/1757972/jem_20160462.pdf by guest on 15 March 2025

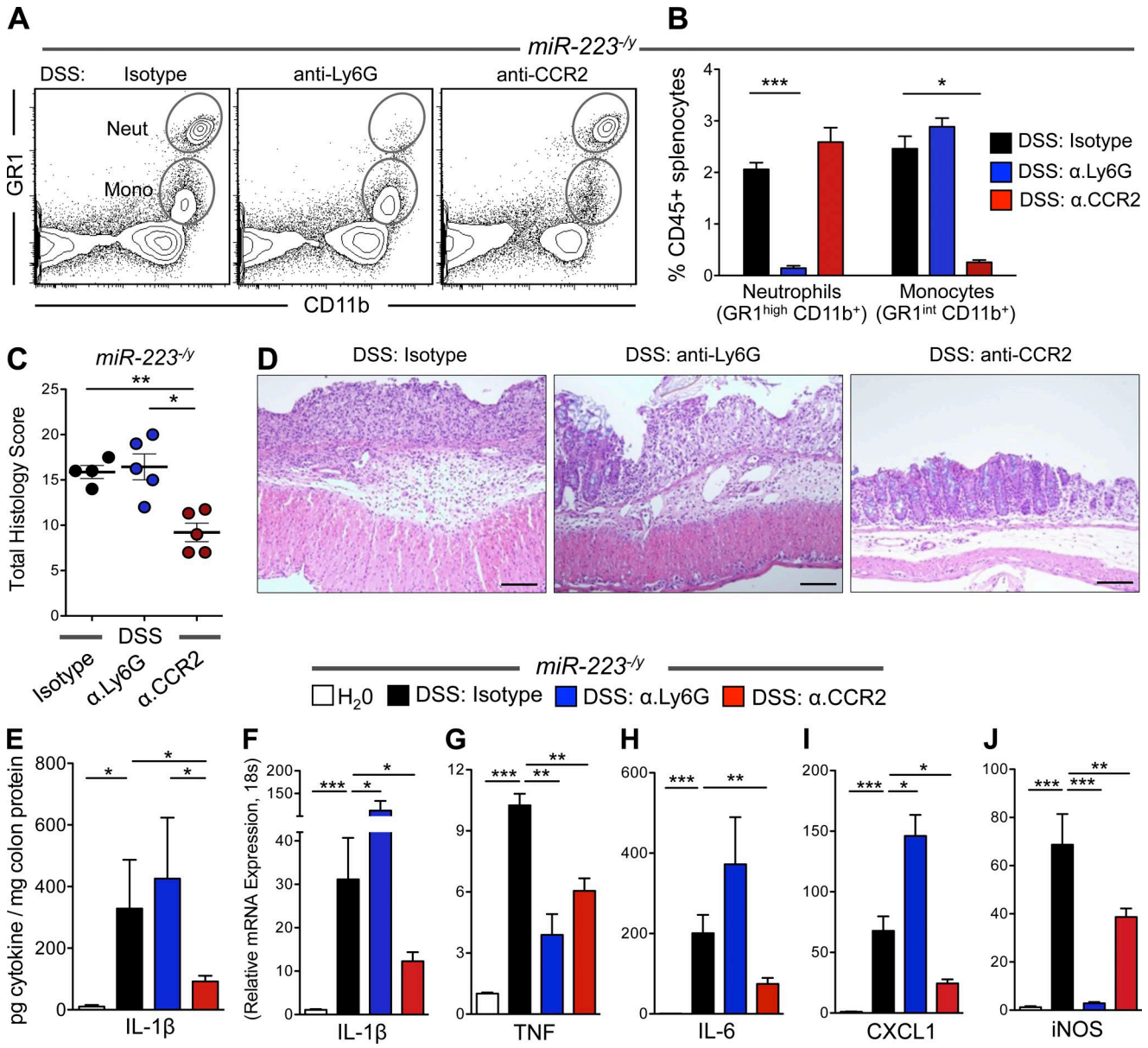

Figure 5. **Depletion of CCR2⁺ monocytes attenuates DSS-colitis and IL-1β in *miR-223*$^{-/y}$ mice.** DSS was administered in drinking water ad libitum (3% wt/vol) for 6 d to *miR-223*$^{-/y}$ mice. Mice were treated on days 0–5 with anti-Ly6G (1A8; 300 µg/d, i.p.), anti-CCR2 (MC21; 20 µg/d, i.p.), or isotype vehicles and euthanized 24 h after the final treatment. (A) Representative flow cytometry analysis from *miR-223*$^{-/y}$ mice subjected to DSS (3% wt/vol; day 2). (B) Neutrophils were identified as live, CD45⁺ singlets, SSC-A^{high} GR1^{high} CD11b⁺; monocytes were identified as live, CD45⁺ singlets, SSC-A^{high} GR1^{int} CD11b⁺. n = 3 mice/group; statistical significance determined by ANOVA with Newman–Keuls multiple comparison test. (C) Histopathology scores from *miR-223*$^{-/y}$ mice after DSS-colitis. n = 5 mice/group; statistical significance determined by ANOVA with Newman–Keuls multiple comparison test. (D) Representative micrographs of colon H&E from *miR-223*$^{-/y}$ mice after DSS-colitis. (E) IL-1β was measured by ELISA from whole colon tissue. n = 5 mice/group; statistical significance determined by ANOVA with Newman–Keuls multiple comparison test. (F–J) mRNA for IL-1β (F), TNF (G), IL-6 (H), CXCL1 (I), and iNOS (J) was assessed by QPCR from whole colon tissue. n = 4–5 mice/group; statistical significance determined by ANOVA with Newman–Keuls multiple comparison test. Data are expressed as mean ± SEM; *, P < 0.05; **, P < 0.01; ***, P < 0.001 versus the indicated counterpart from two independent experiments. Bars, 100 µm.

however no structural motifs are found in this area by the algorithm RegRNA (http://regrna2.mbc.nctu.edu.tw/) except for a GY-box that is actually within the miR-223 binding site (Huang et al., 2006). Thus removal of NLRP3 inhibition by miR-223 is likely to be the dominant functional effect in this strain of mice. These mice were then crossed with CMV-Cre mice to globally knock out the miR-223 target site (*Nlrp3*^{m223del}; Fig. S2). To determine the absolute regulation of NLRP3 by miR-223, we analyzed NLRP3 expression and NLRP3 inflammasome activity in neutrophils

Downloaded from http://rupress.org/jem/article-pdf/214/6/1737/1757972/jem_20160462.pdf by guest on 15 March 2025

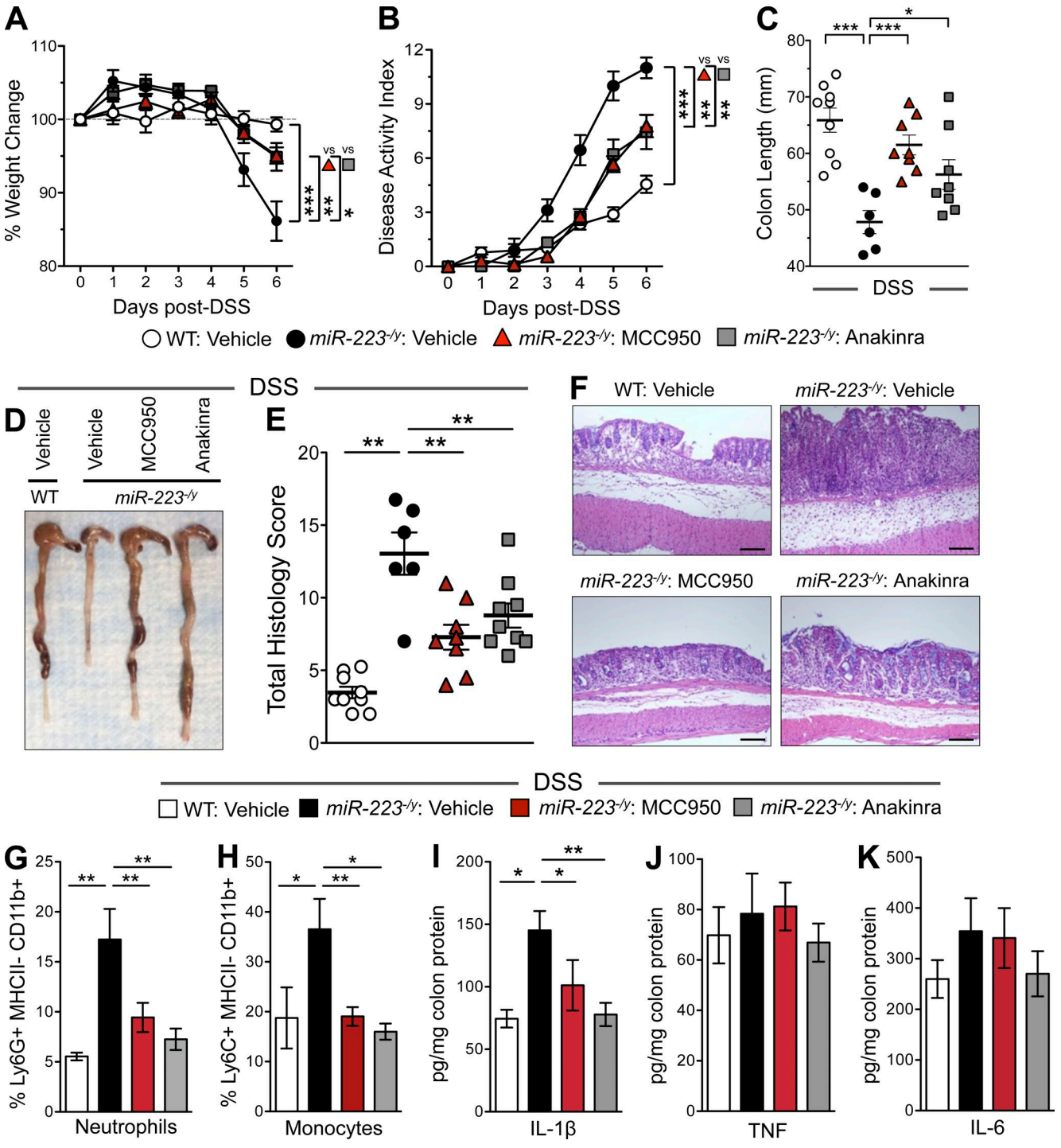

Figure 6. **Inhibition of NLRP3 or IL-1β attenuates DSS-colitis in *miR-223*$^{-/y}$ mice.** DSS was administered in drinking water ad libitum (3% wt/vol) for 6 d to WT and *miR-223*$^{-/y}$ mice. *miR-223*$^{-/y}$ mice received the small molecule inhibitor of NLRP3, MCC950 (20 mg/kg/d, i.p.); the IL-1 receptor antagonist, anakinra (20 mg/kg/d, i.p.); or saline vehicle and were euthanized 24 h after the final treatment. (A) Weight loss during colitis was expressed as the percentage of change from day 0. n = 7–9 mice/group; statistical significance determined by ANOVA with Newman–Keuls multiple comparison test. (B) Clinical DAI was a composite of weight changes (percentage of day 0), stool score, and occult blood index. n = 7–9 mice/group; statistical significance determined by ANOVA with Newman–Keuls multiple comparison test. (C) Colon lengths of DSS-treated mice were assessed at the time of necropsy. n = 6–9 mice/group; statistical significance determined by ANOVA with Newman–Keuls multiple comparison test. (D) Representative macroscopic images of colons after treatment. (E) Histopathology scores from WT and *miR-223*$^{-/y}$ colons after DSS-colitis. n = 6–9 mice/group; statistical significance determined by ANOVA with Newman–Keuls multiple comparison test. (F) Representative micrographs of colon H&E from WT and *miR-223*$^{-/y}$ mice after treatment. (G and

Downloaded from http://rupress.org/jem/article-pdf/214/6/1737/1757972/jem_20160462.pdf by guest on 15 March 2025

from *Nlrp3*^{m223del} mice stimulated with LPS and nigericin to activate the NLRP3 inflammasome. A consistent increase in NLRP3 expression was observed in resting and LPS-stimulated knockout neutrophils (del/del) compared with WT (+/+; Fig. 7 A). Compared with WT controls, there was a marked increase in the production of mature IL-1β in homozygous knockout neutrophils (Fig. 7 B) with no significant difference in TNF (Fig. 7 C). Furthermore, although miR-223 mimics transfected into WT (+/+) monocytes repressed NLRP3, *Nlrp3*^{m223del} (del/del) monocytes were refractory to this treatment (Fig. S3). Collectively, these data confirm that we have generated mice in which NLRP3 is no longer inhibited by myeloid-derived miR-223.

We next tested the functional consequence on experimental colitis in vivo. We found that *Nlrp3*^{m223del} mice were more susceptible to DSS-colitis, as indicated by an increase in infiltrating neutrophils in addition to increased weight loss, reduced colon length, and higher histology score (Fig. 7, D–H). Thus, our collective data underscore that in vivo, NLRP3 is the bone fide target of miR-223, and that this is a critical determinant of intestinal inflammation.

Nanoparticle delivery of an miR-223 mimetic attenuates experimental DSS-colitis

Small molecules targeting the pathways involved in aberrant inflammation are the focus of intense investigation for the treatment of IBD. Currently, although the first-in-class miRNA oligonucleotide therapeutic (Miravirsen) demonstrates efficacy in clinical trials for hepatitis C (Janssen et al., 2013), there is no therapeutic application of miRNAs for IBD. Based on our data, we sought to investigate the efficacy of using miR-223 mimetics as a novel therapeutic intervention during experimental colitis. Synthetic murine miR-223 mimics were delivered to mice in nanoparticle lipid emulsion (i.v.; on days 1 and 3 after DSS administration). As a relevant control, we used a corresponding miRNA control that is restrictively expressed in *Caenorhabditis elegans* nematode (Cel-miR-239b). As shown in Fig. 8 A, therapeutic intervention with synthetic miR-223 mimics produced a threefold increase in colonic miR-223 expression during peak disease (day 6 after DSS). This was accompanied by a marked protection from DSS-colitis as indicated by attenuated occult bleeding, weight loss, and edema (Fig. 8, B–E). Furthermore, mmu-miR-223 mimic treatment repressed the miR-223 target, NLRP3, at both mRNA and protein levels (Fig. 8, F and G). This was accompanied by attenuated IL-1β protein and repression of IL-1β, IL-6, TNF, and CXCL1 mRNA transcripts (Fig. 8, H and I). Collectively, these data confirm a critical role for miR-223 during aberrant intestinal inflammation and represent a proof-of-principle therapeutic study using miRNA mimetics to treat experimental IBD.

DISCUSSION

The resident and infiltrating subsets of myeloid cells that populate the intestine play dual roles in intestinal immunity, with the capacity to protect from commensal overstimulation while acting as provocateurs in immune-mediated conditions such as IBD. Although the etiology of IBD remains elusive (with genetic, environmental, and immune components), prevailing hypotheses propose that damage to the intestinal mucosa occurs as a result of a dysregulated innate immune response triggered by microbial antigens (Fiocchi, 1998; Nagler-Anderson, 2001). The NOD-like receptor family, pyrin domain-containing protein 3 (NLRP3) inflammasome is critical for the processing and release of active IL-1β and IL-18 and is rapidly emerging as a crucial regulator of intestinal homeostasis (Zaki et al., 2011; Haneklaus et al., 2013). Thus, understanding the molecular regulation of the inflammasome complex and its dysregulation during aberrant inflammation in IBD is an attractive avenue for therapeutic development.

Because of the ability of IL-1β and IL-18 to drive robust proinflammatory responses, they are tightly regulated at multiple levels to avoid excessive tissue damage. However, the role of the NLRP3 inflammasome in acute intestinal inflammation is controversial, with multiple conflicting studies identifying opposing functions during experimental colitis. A series of studies demonstrated that mice deficient in inflammasome components, NLRP3, caspase-1, or apoptosis-associated speck-like protein containing a CARD (ASC), have heightened susceptibility to DSS-colitis (Allen et al., 2010; Zaki et al., 2010; Song-Zhao et al., 2014). Conversely, another study revealed protective responses in *Nlrp3*$^{-/-}$ mice using the same model (Bauer et al., 2010), whereas pharmacologic inhibition of either caspase-1 or inflammasome activation dampened chronic colitis in *IL-10*$^{-/-}$ mice (Zhang et al., 2014). Although some of these discrepancies across multiple studies may be explained by experimental design and microbiome differences, they highlight a need to further define the molecular regulation of aberrant cytokine stimulation in the intestine. One possible explanation lies in the respective roles of IL-1β versus IL-18 to drive both inflammation and repair (Bamias et al., 2012; Lopetuso et al., 2013).

Indeed, a role for the proinflammatory cytokine IL-1β in the pathogenesis of IBD has been controversial. Increased levels of IL-1β were found in colonic biopsies and isolated myeloid cells, correlating with disease severity (Ligumsky et

H) Flow cytometry–characterized collagenase digested colons for the presence of live, CD45$^+$ CD11b$^+$ myeloid cells that were neutrophils (Ly6G$^+$ MHCII$^-$; G) and monocytes (Ly6C$^+$ MHCII$^-$; H). *n* = 3–5 mice/group; statistical significance determined by ANOVA with Newman–Keuls multiple comparison test. (I–K) Inflammatory cytokine expression was quantified in whole colon tissues from WT or *miR-223*$^{-/y}$ mice after treatment by LEGENDplex bead array (see Materials and methods). *n* = 5–7 mice/group; statistical significance determined by ANOVA with Newman–Keuls multiple comparison test. Data are expressed as mean ± SEM; *, P < 0.05; **, P < 0.01; ***, P < 0.001 versus the indicated counterparts from two independent experiments. Bars, 100 µm.

Downloaded from http://rupress.org/jem/article-pdf/214/6/1737/1757972/jem_20160462.pdf by guest on 15 March 2025

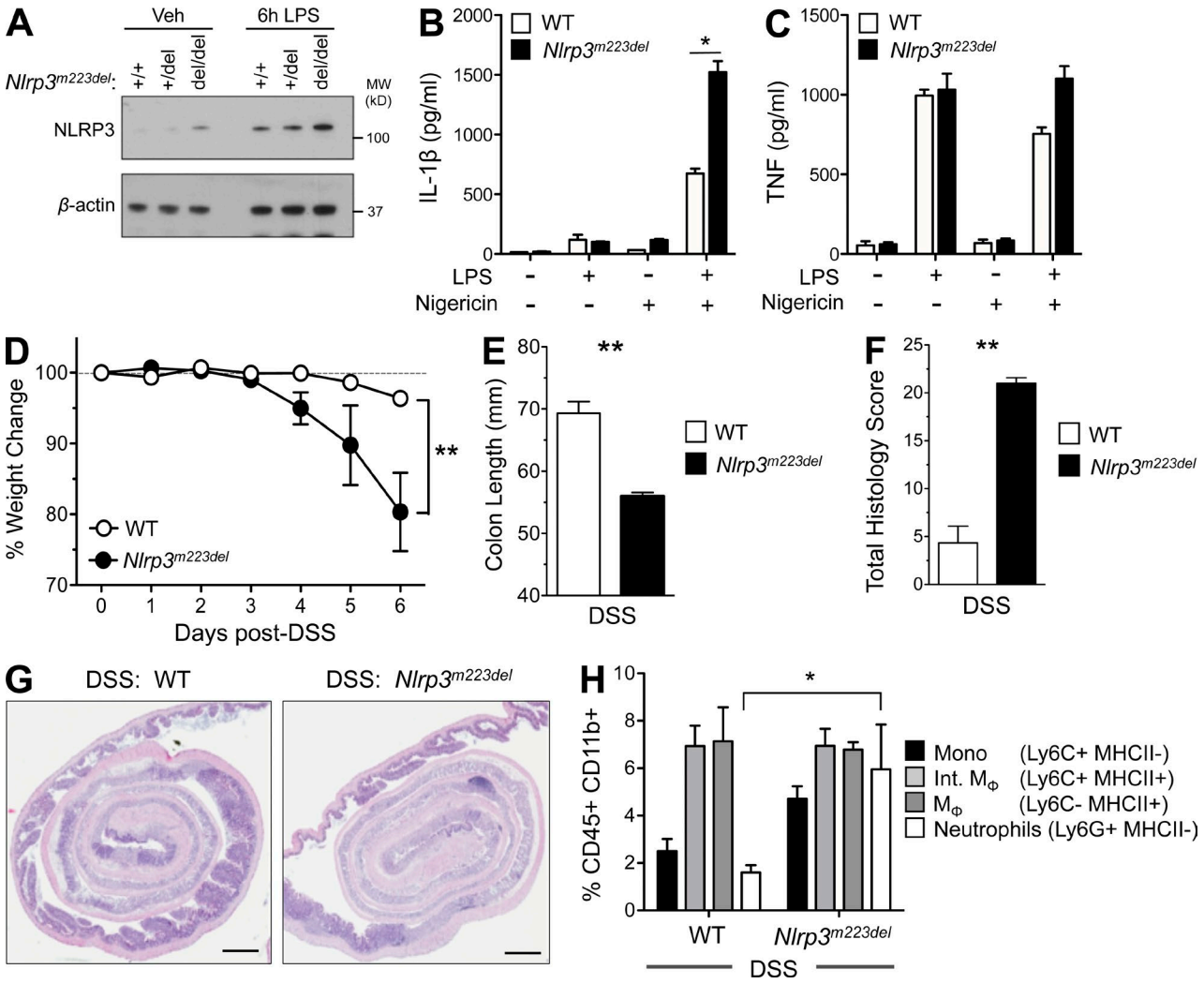

Figure 7. ***Nlrp3***^{m223del} **mice display increased NLRP3 activation in vitro and susceptibility to DSS-colitis.** (A) Neutrophils were cultured ex vivo from WT (+/+) or *Nlrp3*^{m223del} (del/del) mice and stimulated with LPS (1 or 100 ng/ml) for 3 h, as indicated. Samples were lysed in SDS loading buffer and NLRP3, and β-actin protein expression was analyzed by Western immunoblot. Representative immunoblot from three independent mice. (B and C) Neutrophils were cultured with LPS (100 ng/ml) for 3 h, followed by 3 h with nigericin (10 mM), and supernatants were collected for IL-1β (B) or TNF (C) measurement by ELISA. $n = 4$ mice/group; statistical significance determined by unpaired Student's t test. DSS was administered in drinking water ad libitum (3% wt/vol) for 6 d to WT and *Nlrp3*^{m223del} mice. (D) Weight loss during colitis was expressed as the percentage of change from day 0. $n = 3$ mice/group; statistical significance determined by unpaired Student's t test. (E) Colon lengths were assessed at the time of necropsy from WT and *Nlrp3*^{m223del} mice after DSS. $n = 3$ mice/group; statistical significance determined by unpaired Student's t test. (F) Histopathology scores from WT and *Nlrp3*^{m223del} colons after DSS. $n = 3$ mice/group; statistical significance determined by unpaired Student's t test. (G) Representative micrographs of colon H&E from WT and *Nlrp3*^{m223del} mice after DSS-colitis. (H) The frequencies of monocytes, macrophages, and neutrophils were analyzed in WT and *Nlrp3*^{m223del} mice by flow cytometry as a percentage of myeloid cells (gated on CD45$^+$ CD11b$^+$ cells) in the colon at day 2 after DSS treatment. $n = 3$ mice/group; statistical significance determined by unpaired Student's t test. Data are expressed as mean ± SEM; *, $P < 0.05$; **, $P < 0.01$ versus the indicated counterparts. Data are representative of two independent experiments with three to four mice per group. Bars, 1 mm.

al., 1990; Reinecker et al., 1993; Casini-Raggi et al., 1995). Although early studies demonstrated that low-dose recombinant IL-1β protected from the induction of experimental colitis (Cominelli et al., 1990), more recent data have established that inflammatory monocytes and monocyte-derived IL-1β play a major role in driving pathology in DSS-colitis (Seo et al., 2015). This is exemplified by protection from acute DSS-colitis in *IL-1β*$^{-/-}$ and *CCR2*$^{-/-}$ mice or by antibody depletion of CCR2$^+$ monocytes (Andres et al., 2000; Zigmond et al., 2012; Seo et al., 2015). In support of these findings, Shouval et al. (2016) reported a marked improvement in two IL-10R$^{-/-}$ patients with severe and treatment-refractory infant-onset IBD after treatment with IL-1ra (anakinra).

Likewise, with respect to IL-18, recent landmark studies have demonstrated that nonhematopoietic IL-18 plays a reparative role after epithelial damage during DSS-colitis. Both

Downloaded from http://rupress.org/jem/article-pdf/214/6/1737/1757972/jem_20160462.pdf by guest on 15 March 2025

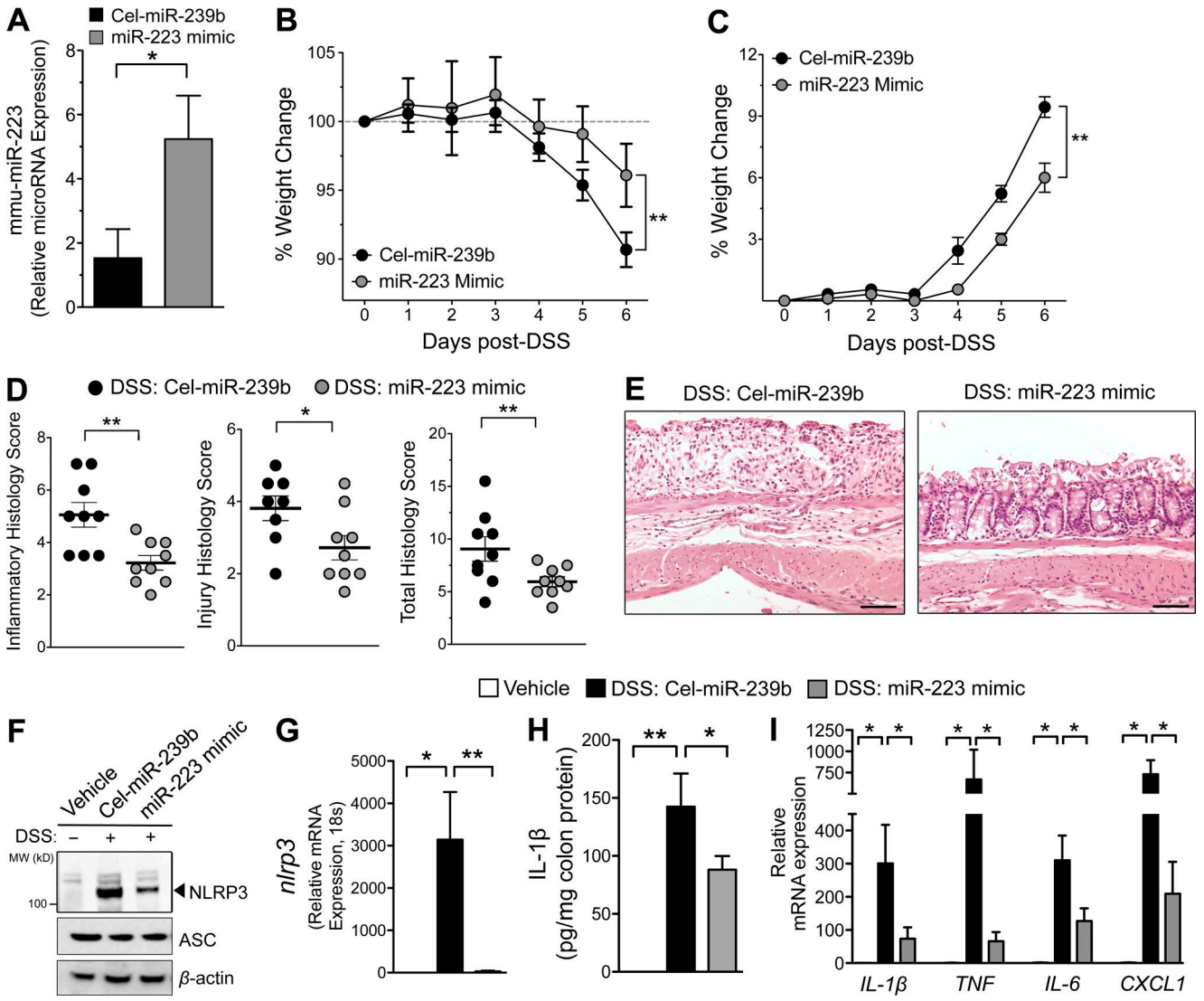

Figure 8. **Nanoparticle delivery of an miR-223 mimetic attenuates experimental DSS-colitis.** DSS was administered in drinking water ad libitum (3% wt/vol) for 6 d to WT mice. Mice were treated with 50 µg (via retro-orbital injection) of either control (Cel-miR239b) or miR-223 mimetic in a nanoparticle solution on days 1 and 3 after DSS administration. (A) miR-223 expression was measured in whole colon tissue by QPCR on day 4 after DSS. (B) Weight loss during treatment was expressed as the percentage of change from day 0. $n = 9$ mice/group; statistical significance determined by unpaired Student's t test. (C) Clinical DAI was a composite of weight changes (percentage of day 0), stool score, and bleeding index. $n = 9$ mice/group; statistical significance determined by unpaired Student's t test. (D) Colonic histopathology scores after treatment. $n = 9$ mice/group; statistical significance determined by unpaired Student's t test. (E) Representative micrographs of colon H&E from treated mice after DSS-colitis. (F) Western immunoblot assessment of NLRP3, ASC, and β-actin in whole colon biopsies. Representative immunoblots from three independent mice. (G) Relative mRNA was assessed by quantitative PCR for NLRP3. $n = 3$–5 mice/group; statistical significance determined by unpaired Student's t test. (H) ELISA measurement of IL-1β whole colon biopsies. $n = 3$–5 mice/group; statistical significance determined by unpaired Student's t test. (I) Relative mRNA was assessed by QPCR for IL-1, TNF, IL-6, and CXCL1 in whole colon tissues. $n = 3$–5 mice/group; statistical significance determined by unpaired Student's t test. Data are expressed as mean ± SEM; *, $P < 0.05$; **, $P < 0.01$ versus the indicated counterpart from two independent experiments. Bars, 100 µm.

nlrp3$^{-/-}$ and *casp1*$^{-/-}$ mice present with enhanced susceptibility to colitis, and treatment of *casp1*$^{-/-}$ mice with recombinant IL-18 can rescue this pathology (Zaki et al., 2010, 2011). In contrast, inhibition of IL-18 has been shown to confer protection in experimental colitis, supporting a procolitogenic role for IL-18. This is elegantly illustrated by protection from DSS-colitis in mice with selective deletion of IL-18 or its receptor IL-18R1 in intestinal epithelial cells (Nowarski et al., 2015). Conversely, deletion of the IL-18 negative regulator, IL-18bp, resulted in severe colitis associated with loss of goblet cells (Nowarski et al., 2015).

It is worth noting that a confounding factor to the interpretations of these discrepant studies lies in the effects of IL-18 on the microbiome, where an outgrowth of pathogenic

Downloaded from http://rupress.org/jem/article-pdf/214/6/1737/1757972/jem_20160462.pdf by guest on 15 March 2025

intestinal microbial communities is observed in *IL-18*$^{-/-}$ mice (Elinav et al., 2011; Henao-Mejia et al., 2012). Furthermore, although DSS-colitis represents a model of acute injury that is self-limiting, varied courses of DSS administration and concentrations (~2–6% wt/vol) will invariably confound the extrapolation of this work to the clinical setting. DSS-induced epithelial cell death releases alarmins such as IL-1α that initiate and exacerbate the inflammatory response (Bersudsky et al., 2014). As such, heightened epithelial cell death or chronic periods of active inflammation, without allowing for reparative signaling in the mucosa, will present with altered cytokine kinetics compared with acute and limited insults. We observed no role for miR-223 in nonhematopoietic cells (Fig. 2) and the levels of IL-1α and IL-18 were comparable in WT and *miR-223*$^{-/y}$ mice after the initiation of acute DSS-colitis (Fig. 3). As such, our data using three different model systems of miR-223 deficiency (*miR-223*$^{-/y}$, *miR-223*$^{-/y}$ chimeras, and *Nlrp3*^{m223del}) suggest that the influx of myeloid cells with heightened and prolonged release of mature IL-1β may override any protective effect of IL-18 on the epithelium. This role for excessive myeloid-driven inflammation is supported by protection from acute DSS-colitis in *IL-1β*$^{-/-}$ and *CCR2*$^{-/-}$ mice or by antibody depletion of CCR2^{+} monocytes (Andres et al., 2000; Zigmond et al., 2012; Seo et al., 2015). In addition, we provide data that selective pharmacologic blockade of NLRP3 (MCC950), IL-1β inhibition (anakinra), or nanoparticle delivery of miR-223 mimetics exhibit a marked and protective effect during the course of acute colitis.

Within the myeloid lineage, miR-223 is lowest in mature, tissue-resident macrophages but higher in circulating monocytes and neutrophils (Johnnidis et al., 2008; Bauernfeind et al., 2012; Haneklaus et al., 2012). Although our data and the current literature indicate a proinflammatory role for monocytes infiltrating the inflamed colon during DSS-colitis, NLRP3 is expressed in several other myeloid-derived cells, and thus miR-223–NLRP3 interactions may have cell and tissue intrinsic effects in different disease states or infections. The miR-223–NLRP3 interaction is particularly important in neutrophils. For example, miR-223 expression is highest in human and mouse neutrophils compared with macrophages (Ramkissoon et al., 2006; Johnnidis et al., 2008), and neutrophils have a functional NLRP3 inflammasome (Mankan et al., 2012; Karmakar et al., 2015). The enhanced secretion of IL-1β with miR-223 deficiency may also drive IL-1β–mediated expression of chemokines CXCL1, CXCL2, and CCL2 from a multitude of cellular sources and plays a direct role in the recruitment of neutrophils and monocytes into inflamed tissues (Calkins et al., 2002), thus agreeing with our observation of increased neutrophils and monocytes in the inflamed colons of miR-223–deficient mice or *Nlrp3*^{m223del} mice in which NLRP3 is no longer regulated by miR-223. In addition, a direct role for miR-223 on CXCL2 has been observed in the setting of tuberculosis, and this may have an additive role during DSS-colitis in *miR-223*$^{-/y}$ mice (Dorhoi et al., 2013).

Collectively, our studies highlight the miR-223–NLRP3–IL-1β regulatory circuit as a critical component of intestinal inflammation. miR-223 serves to constrain the level of NLRP3 activation and provides an early break, limiting cytokine-mediated immune disequilibrium. Thus, as miR-223 can restrain pathological intestinal inflammation, genetic or pharmacologic stabilization of miR-223 may hold promise as a future novel therapeutic modality for active flares in IBD.

MATERIALS AND METHODS

Human subjects

The institutional review board of the University of Colorado Denver approved all human studies. CD and UC patients were diagnosed using established criteria and CD phenotype per the Montreal criteria (Satsangi et al., 2006; see Table 1 for patient characteristics). Patient demographics and medications were recorded at the time of endoscopic evaluation, during which mucosal biopsies were obtained. The determination of disease activity was based on endoscopic evidence of mucosal inflammation.

Mouse strains

miR-223$^{-/y}$ mice on a C57BL/6J background were provided by V. Dawson (Johns Hopkins University, Baltimore, MD) and bred in-house. CD45.1 (B6.SJL-*Ptprc*^{a}*Pep3*^{b}/BoyJ) were purchased from The Jackson Laboratory. C57BL/6J (CD45.2) mice were bred in-house. Experimental mice were housed separately according to genotype (i.e., B6.WT vs. *miR-223*$^{-/y}$), matched for age and sex, and typically 8–12 wk of age. In one series of studies (Fig. S1), WT and *miR-223*$^{-/y}$ mice were cohoused from weaning (21 d), and experimental colitis

Table 1. **Clinical characteristics of study subjects**

Phenotype	*n*	Age (mean)	Disease duration (mean)	Current IBD medications		
				Prednisone	AZA/6MP	Anti-TNF
		yr	*yr*			
Healthy controls	10	51.4	NA	0%	0%	0%
Inactive UC	6	47.8	16.8	33%	50%	0%
Active UC	6	51.5	8.8	50%	33%	0%
Inactive Crohn's	4	47.5	22.0	0%	17%	33%
Active Crohn's	6	36.7	5.0	33%	0%	0%

NA, not applicable.

Downloaded from http://rupress.org/jem/article-pdf/214/6/1737/1757972/jem_20160462.pdf by guest on 15 March 2025

was induced at 8 wk of age. All mice were bred under specific pathogen–free conditions, and fecal samples were negative for *Helicobacter* species, protozoa, and helminthes. Animal procedures were approved by the Institutional Animal Care and Use Committees at the University of Colorado Denver and the Walter and Eliza Hall Institute of Medical Research/University of Melbourne.

Generation of the *Nlrp3^{m223del}* mouse

Mice lacking the miR-223 target site in the Nlrp3 3′ UTR were generated by Ingenious targeting laboratory (Ronkonkoma, NY) on a C57BL/6 background. Two loxP sites were introduced flanking 100 bp in the Nlrp3 locus that contain the miR-223 target site, 5′-*ATAACTTCGTATAGCATACATTATACGAAGTTAT*CTGGGCCTCTGGTTTTTTGACCTTTGCCCATACCTTCAGTCTTGTCTTCCTGTTAACTGACCATCCCGCATAAGGAGCTGCCCGTGGGC*ATAACTTCGTATAGCATACATTATACGAAGTTAT*-3′ (loxP sites in italics and miR-223 target site underlined). In addition, a biotinylation reporter sequence (BirA) recognition site, 5′-ATGGCCAGCAGCCTCAGACAGATCCTCGACAGCCAGAAGATGGAGTGGAGAAGCAACGCCGGCGGCAGC-3′ (coding for MASSLRQILDSQKMEWRSNAGGS), was added to the 3′ end of the Nlrp3 coding region. Transgenic mice were crossed with CMV-Cre mice (The Jackson Laboratory) to delete the miRNA target site. All animal experiments were performed under the standards of, and were approved by, the Walter and Eliza Hall Institute Animal Ethics Committee.

Generation of BM chimeric mice

Femurs and tibias from WT (CD45.1 or CD45.2) and *miR-223$^{-/y}$* (CD45.2) donor mice were removed and flushed through a 70-µm cell strainer with cold RPMI 1640 to harvest BM cells. Recipient mice (8–12 wks of age) were irradiated with a total dose of 1,000 rads (500 rads twice, 4 h apart). Immediately after irradiation, 1×10^7 BM cells/mouse were intravenously injected via the retro-orbital route in 0.1 ml 0.9% sodium chloride. Mice were housed in microisolator cages for 8 wks to recover before induction of DSS-colitis. To assess BM reconstitution, spleens were excised at necropsy, and red blood cells were lysed, followed by flow cytometry for $CD45^+$ leukocytes expressing either CD45.1 (clone A20) or CD45.2 (clone 104; eBioscience).

Induction of experimental DSS-colitis and treatment studies

DSS (3% wt/vol, 36,000–50,000 kD; MP Biomedicals) was administered in drinking water ad libitum for 6 d. DSS solution was replaced once on day 3. Examination for clinical signs of colitis (i.e., weight loss, stool consistency, and fecal blood) were performed and recorded daily. A colitis DAI was calculated for each mouse daily, based on body weight loss, occult blood, and stool consistency. A score of 1–4 was given for each parameter (0: no weight loss, normal stool, no blood; 1: 1–3% weight loss; 2: 3–6% weight loss, loose stool, blood visible in stool; 3: 6–9% weight loss; 4: >9% weight loss, diarrhea, gross bleeding), with a maximum DAI score of 12. Loose stool was defined as the formation of a stool pellet that readily loses consistency upon handling. Diarrhea was defined as no pellet formation. Gross bleeding was defined as fresh perianal blood with obvious hematochezia. Upon necropsy, colon length was additionally measured.

To deplete neutrophils during DSS-colitis, *miR-223$^{-/y}$* mice were treated i.p. with 300 µg anti-Ly6G (1A8) or isotype control daily from days 0–5. To deplete monocytes, *miR-223$^{-/y}$* mice were treated i.p. with 20 µg anti-CCR2 (MC21) or isotype control daily from days 0–5 after DSS. Mice were euthanized 24 h after the terminal treatment.

To inhibit the NLRP3 inflammasome in vivo, *miR-223$^{-/y}$* mice were treated i.p. with 20 mg/kg MCC950 (Coll et al., 2015) or saline vehicle daily on days 0–5 of DSS treatment. To block IL-1β in vivo, *miR-223$^{-/y}$* mice were treated i.p. with 20 mg/kg of anakinra or a saline vehicle daily on days 0–5 of DSS treatment. Mice were euthanized 24 h after the last treatment on day 6 after DSS.

Tissue fixation, paraffin embedding, and histological scoring

Colons were excised, opened longitudinally, and washed with cold PBS followed by fixation with 10% buffered formalin. Tissue was embedded in paraffin, cut into 5-µm sections, and stained with hematoxylin and eosin (H&E). Histological assessment of colitis was performed by a board-certified pathologist, who was blinded to experimental details, as previously described (McNamee et al., 2010).

Isolation, culture, and treatment of mouse BMDMs and neutrophils

Mouse BM from femurs and tibias was resuspended in HBSS-EDTA, and BMDMs were isolated, cultured, and activated for 5 d as previously described (Mosser and Zhang, 2008). For NLRP3 inflammasome activation, 10^6 cells/ml BMDM were treated with LPS (100 ng/ml) for 3 h followed by ATP (1 mM; InvivoGen) for 3 h or vehicle controls. For neutrophil isolation, BM was resuspended in HBSS-EDTA and layered on a Percoll gradient (52, 69, and 78%) in 1× HBSS. Neutrophils were removed from the 69/72% interphase. Cells were washed twice with HBSS and seeded at 10^6 cells/ml in OptiMEM supplemented with 1 µg/ml aprotinin. NLRP3 was activated by 3-h LPS priming (100 ng/ml) followed by 3-h stimulation with 10 µM nigericin. After the combined treatments, cell-free supernatants were harvested, and cells were washed and harvested for either mRNA or protein extraction and analysis.

For functional studies assessing the role of miR-223 in the Nlrp3 binding site–deficient mice, primary monocytes were isolated using anti-CD14 magnetic beads from WT or *nlrp3^{m223del}* BM (Miltenyi Biotec) and differentiated by incubation with 100 ng/ml M-CSF for 3 d. Primary monocytes were transfected with 25 nM control scrambled or miR-223 mimic using Dharmafect reagent 3 (Thermo Fisher Scien-

Downloaded from http://rupress.org/jem/article-pdf/214/6/1737/1757972/jem_20160462.pdf by guest on 15 March 2025

tific) and activated with 1 µg/ml LPS and 5 mM ATP (Sigma-Aldrich) as previously described (Haneklaus et al., 2012).

Leukocyte isolation and flow cytometry

Colons were excised, opened longitudinally, and washed with cold PBS followed by incubation with IEL solution (PBS, 15 mmol/L Hepes, and 1 mmol/L EDTA) to remove epithelial cells. Colons were cut into ∼1-cm pieces and then enzymatically digested (RPMI, 2% FCS, 15 mmol/L Hepes, 200 U/ml collagenase VIII [Sigma-Aldrich], and 1 µg/ml DNase [Thermo Fisher Scientific]) at 37°C with gentle agitation for ∼30 min. Debris was extracted using a 100-µM filter, and the cell suspension was washed with cold RPMI/10% FBS twice. Cells from indicated compartments were incubated with fluorescently labeled anti-mouse antibodies against MHC II (M5/114.15.2), CD11b (M1/70), CD11c (N418), Ly6G (1A8), Ly6C (HK1.4), CD45 (30-F11), CD115 (AFS98; eBioscience, San Diego, CA), or corresponding isotype controls. Dead cells were excluded using a Live/Dead Fixable Aqua Stain (Invitrogen), and flow cytometry was performed using a BD FACSCanto II (BD). Further analyses were performed using FLOWJo software (Tree Star).

miRNA and mRNA transcriptional analysis

Total RNA or separated fractions of miRNA and mRNA were isolated from colon tissue using Qiazol Reagent and an RNeasy kit according to the manufacturer's instructions (Qiagen). Transcript levels were determined by real-time RT-PCR using specific primer sets (miRNA, Qiagen; mRNA, Taqman, Applied Biosystems). Expression levels of miRNAs were normalized to endogenous RNU-6, whereas 18s was used to normalize mRNA expression profiles.

Western immunoblot analysis of NLRP3, IL-1β, and ASC

To measure NLRP3, ASC and IL-1β protein content, pelleted BMDMs, neutrophils, or colon biopsies were freeze-thawed in T-Per Tissue Protein Extraction Reagent with Pierce Phosphatase and Protease Inhibitor (Thermo Fisher Scientific). Supernatant protein concentration was quantified using Pierce BCA Protein Assay kit (Thermo Fisher Scientific), resuspended in reducing 4× Laemmli sample buffer (Bio-Rad) and heated to 98°C for 10 min. Samples were resolved on a 10% polyacrylamide gel and semi-dry transferred to nitrocellulose membranes. The membranes were blocked for 30 min at room temperature in TBS-T supplemented with 5% blotting-grade nonfat milk (Bio-Rad). Membranes were subsequently incubated with rabbit anti-mouse NLRP3 (D4D8T; Cell Signaling Technology) at a concentration of 1:150, rabbit anti-mouse ASC (N-15; Santa Cruz Biotechnology, Inc.) at a concentration of 1:500, or goat anti-mouse IL-1β (AF-401-NA; R&D Systems) at a concentration of 1:200 overnight at 4°C. After three 15-min washes in TBS-T, NLRP3, ASC, and IL-1β membranes were incubated in goat anti–rabbit IgG-HRP secondary Ab (Santa Cruz Biotech) or bovine anti–goat IgG-HRP secondary Ab (Santa Cruz Biotechnology, Inc.) at concentrations of 1:2,000 to 1:5,000 for 2 h at room temperature. Membranes were washed in TBS-T, and proteins were detected by enhanced chemiluminescence (Thermo Fisher Scientific). To control for protein loading, blots were stripped and reprobed for β-actin (I-19; Santa Cruz Biotechnology, Inc.) and a bovine anti–goat IgG-HRP secondary Ab (Santa Cruz Biotechnology, Inc.).

Cytokine analysis from intestinal tissues and cell culture supernatant

Cytokine analysis was performed on colon intestinal tissue or cell culture supernatants using mouse IL-18 Platinum ELISA kits (eBioscience), Duoset mouse IL-1β and TNF ELISA kits (R&D Systems), and LEGENDplex Mouse Inflammation panel (13-plex; BioLegend) according to the manufacturers' instructions.

In vivo nanoparticle delivery of mmu-miR-223 mimetic

To use a pharmacological approach to overexpress mmu-miR-223 during experimental DSS-colitis, a nanoparticle-based approach was used to transport synthetic mmu-miR-223. NLE consists of 1,2-dioleoyl-sn-glycero-3-phosphocholine, squalene oil, polysorbate 20, and an antioxidant that, in complex with synthetic miRNAs, form nanoparticles in the nanometer diameter range. Mice were treated i.v., via retro-orbital route (days 1 and 3 after DSS) with a dose of 50 µg synthetic mmu-miR-223 (mimic-223; Dharmacon) or respective control (Cel-miR-239b) formulated with NLE according to the manufacturer's instructions (MaxSuppressor In Vivo RNA-LANCEr II; Bioo Scientific).

Statistical analysis

Statistical analyses were performed using ANOVA or two-tailed Student's *t* test. Data were expressed as mean ± SEM. Statistical significance was set at $P < 0.05$.

Online supplemental material

Fig. S1 shows clinical and histopathology data for a DSS-colitis study using either single or cohoused WT and *miR-223*$^{-/y}$ mice. Fig. S2 shows a schematic representation for the development of the *nlrp3*^{m223del} mouse. Fig. S3 demonstrates that BMDM from *nlrp3*^{m223del} mice are refractory to repression of Nlrp3 with miR-223 mimetics.

ACKNOWLEDGMENTS

The authors thank Valina Dawson (Johns Hopkins University) for kindly providing *miR-223*$^{-/y}$ mice, Kayla Schwisow for technical assistance with human colonic biopsies, and Melissa Ledezma for technical assistance with animal husbandry.

The work was supported by the German Research Foundation (DFG) and the American Heart Association (AHA) to V. Neudecker; National Institutes of Health grant K01DK106315 and NASPGHAN Foundation/Crohn's and Colitis Foundation of America (CCFA) grant 3760 to J.C. Masterson; National Institutes of Health grants R01 DK097075, R01- HL098294, POI-HL114457, R01-DK082509, R01-HL109233, R01-DK109574, R01-HL119837, and R01-HL133900 to H.K. Eltzschig; Australian National Health and Medical Research Council project grants 1057815 and 1099262 and Independent Research Institutes Infrastructure Support Scheme grant 361646, fellowships from the Victorian Endowment for Science Knowledge and Innovation, a

Downloaded from http://rupress.org/jem/article-pdf/214/6/1737/1757972/jem_20160462.pdf by guest on 15 March 2025

State Government of Victoria Operational Infrastructure Support Grant, and funding from GlaxoSmithKline to S.L. Masters; and CCFA grants 273007 and 409992 to E.N. McNamee.

The authors declare no competing financial interests.

Author contributions: V. Neudecker, H.K. Eltzschig, and E.N. McNamee conceived of and designed the project. V. Neudecker, M. Haneklaus, O. Jensen, L. Khailova, J.C. Masterson, H. Tye, K. Biette, P. Jedlicka, K.S. Brodsky, S.L. Masters, and E.N. McNamee designed and performed experiments and analyzed primary data. M.E. Gerich, M. Mack, A.A.B. Robertson, M.A. Cooper, G.T. Furuta, C.A. Dinarello, L.A. O'Neill, H.K. Eltzschig, and S.L. Masters provided essential study materials, reagents, and patient samples. V. Neudecker and E.N. McNamee drafted the initial manuscript. All authors edited the manuscript.

Submitted: 31 March 2016

Revised: 22 January 2017

Accepted: 28 March 2017

REFERENCES

Allen, I.C., E.M. TeKippe, R.M. Woodford, J.M. Uronis, E.K. Holl, A.B. Rogers, H.H. Herfarth, C. Jobin, and J.P. Ting. 2010. The NLRP3 inflammasome functions as a negative regulator of tumorigenesis during colitis-associated cancer. *J. Exp. Med.* 207:1045–1056. http://dx.doi.org/10.1084/jem.20100050

Andres, P.G., P.L. Beck, E. Mizoguchi, A. Mizoguchi, A.K. Bhan, T. Dawson, W.A. Kuziel, N. Maeda, R.P. MacDermott, D.K. Podolsky, and H.C. Reinecker. 2000. Mice with a selective deletion of the CC chemokine receptors 5 or 2 are protected from dextran sodium sulfate-mediated colitis: Lack of CC chemokine receptor 5 expression results in a $NK1.1^+$ lymphocyte-associated Th2-type immune response in the intestine. *J. Immunol.* 164:6303–6312. http://dx.doi.org/10.4049/jimmunol.164.12.6303

Baek, D., J. Villén, C. Shin, F.D. Camargo, S.P. Gygi, and D.P. Bartel. 2008. The impact of microRNAs on protein output. *Nature.* 455:64–71. http://dx.doi.org/10.1038/nature07242

Bamias, G., D. Corridoni, T.T. Pizarro, and F. Cominelli. 2012. New insights into the dichotomous role of innate cytokines in gut homeostasis and inflammation. *Cytokine.* 59:451–459. http://dx.doi.org/10.1016/j.cyto.2012.06.014

Bauer, C., P. Duewell, C. Mayer, H.A. Lehr, K.A. Fitzgerald, M. Dauer, J. Tschopp, S. Endres, E. Latz, and M. Schnurr. 2010. Colitis induced in mice with dextran sulfate sodium (DSS) is mediated by the NLRP3 inflammasome. *Gut.* 59:1192–1199. http://dx.doi.org/10.1136/gut.2009.197822

Bauernfeind, F., A. Rieger, F.A. Schildberg, P.A. Knolle, J.L. Schmid-Burgk, and V. Hornung. 2012. NLRP3 inflammasome activity is negatively controlled by miR-223. *J. Immunol.* 189:4175–4181. http://dx.doi.org/10.4049/jimmunol.1201516

Bersudsky, M., L. Luski, D. Fishman, R.M. White, N. Ziv-Sokolovskaya, S. Dotan, P. Rider, I. Kaplanov, T. Aychek, C.A. Dinarello, et al. 2014. Non-redundant properties of IL-1α and IL-1β during acute colon inflammation in mice. *Gut.* 63:598–609. http://dx.doi.org/10.1136/gutjnl-2012-303329

Brazil, J.C., N.A. Louis, and C.A. Parkos. 2013. The role of polymorphonuclear leukocyte trafficking in the perpetuation of inflammation during inflammatory bowel disease. *Inflamm. Bowel Dis.* 19:1556–1565. http://dx.doi.org/10.1097/MIB.0b013e318281f54e

Calkins, C.M., D.D. Bensard, B.D. Shames, E.J. Pulido, E. Abraham, N. Fernandez, X. Meng, C.A. Dinarello, and R.C. McIntyre Jr. 2002. IL-1 regulates in vivo C-X-C chemokine induction and neutrophil sequestration following endotoxemia. *J. Endotoxin Res.* 8:59–67.

Casini-Raggi, V., L. Kam, Y.J. Chong, C. Fiocchi, T.T. Pizarro, and F. Cominelli. 1995. Mucosal imbalance of IL-1 and IL-1 receptor antagonist in inflammatory bowel disease. A novel mechanism of chronic intestinal inflammation. *J. Immunol.* 154:2434–2440.

Coll, R.C., A.A. Robertson, J.J. Chae, S.C. Higgins, R. Muñoz-Planillo, M.C. Inserra, I. Vetter, L.S. Dungan, B.G. Monks, A. Stutz, et al. 2015. A small-molecule inhibitor of the NLRP3 inflammasome for the treatment of inflammatory diseases. *Nat. Med.* 21:248–255. http://dx.doi.org/10.1038/nm.3806

Cominelli, F., C.C. Nast, R. Llerena, C.A. Dinarello, and R.D. Zipser. 1990. Interleukin 1 suppresses inflammation in rabbit colitis. Mediation by endogenous prostaglandins. *J. Clin. Invest.* 85:582–586. http://dx.doi.org/10.1172/JCI114476

Dorhoi, A., M. Iannaccone, M. Farinacci, K.C. Faé, J. Schreiber, P. Moura-Alves, G. Nouailles, H.J. Mollenkopf, D. Oberbeck-Müller, S. Jörg, et al. 2013. MicroRNA-223 controls susceptibility to tuberculosis by regulating lung neutrophil recruitment. *J. Clin. Invest.* 123:4836–4848. http://dx.doi.org/10.1172/JCI67604

Elinav, E., T. Strowig, A.L. Kau, J. Henao-Mejia, C.A. Thaiss, C.J. Booth, D.R. Peaper, J. Bertin, S.C. Eisenbarth, J.I. Gordon, and R.A. Flavell. 2011. NLRP6 inflammasome regulates colonic microbial ecology and risk for colitis. *Cell.* 145:745–757. http://dx.doi.org/10.1016/j.cell.2011.04.022

Eulalio, A., L. Schulte, and J. Vogel. 2012. The mammalian microRNA response to bacterial infections. *RNA Biol.* 9:742–750. http://dx.doi.org/10.4161/rna.20018

Fiocchi, C. 1998. Inflammatory bowel disease: Etiology and pathogenesis. *Gastroenterology.* 115:182–205. http://dx.doi.org/10.1016/S0016-5085(98)70381-6

Gentner, B., G. Schira, A. Giustacchini, M. Amendola, B.D. Brown, M. Ponzoni, and L. Naldini. 2009. Stable knockdown of microRNA in vivo by lentiviral vectors. *Nat. Methods.* 6:63–66. http://dx.doi.org/10.1038/nmeth.1277

Haneklaus, M., M. Gerlic, M. Kurowska-Stolarska, A.A. Rainey, D. Pich, I.B. McInnes, W. Hammerschmidt, L.A. O'Neill, and S.L. Masters. 2012. Cutting edge: miR-223 and EBV miR-BART15 regulate the NLRP3 inflammasome and IL-1β production. *J. Immunol.* 189:3795–3799. http://dx.doi.org/10.4049/jimmunol.1200312

Haneklaus, M., M. Gerlic, L.A. O'Neill, and S.L. Masters. 2013. miR-223: Infection, inflammation and cancer. *J. Intern. Med.* 274:215–226. http://dx.doi.org/10.1111/joim.12099

Henao-Mejia, J., E. Elinav, C. Jin, L. Hao, W.Z. Mehal, T. Strowig, C.A. Thaiss, A.L. Kau, S.C. Eisenbarth, M.J. Jurczak, et al. 2012. Inflammasome-mediated dysbiosis regulates progression of NAFLD and obesity. *Nature.* 482:179–185. http://dx.doi.org/10.1038/nature10809

Hsu, S.H., B. Wang, J. Kota, J. Yu, S. Costinean, H. Kutay, L. Yu, S. Bai, K. La Perle, R.R. Chivukula, et al. 2012. Essential metabolic, anti-inflammatory, and anti-tumorigenic functions of miR-122 in liver. *J. Clin. Invest.* 122:2871–2883. http://dx.doi.org/10.1172/JCI63539

Huang, H.Y., C.H. Chien, K.H. Jen, and H.D. Huang. 2006. RegRNA: An integrated web server for identifying regulatory RNA motifs and elements. *Nucleic Acids Res.* 34:W429–W434. http://dx.doi.org/10.1093/nar/gkl333

Janssen, H.L., H.W. Reesink, E.J. Lawitz, S. Zeuzem, M. Rodriguez-Torres, K. Patel, A.J. van der Meer, A.K. Patick, A. Chen, Y. Zhou, et al. 2013. Treatment of HCV infection by targeting microRNA. *N. Engl. J. Med.* 368:1685–1694. http://dx.doi.org/10.1056/NEJMoa1209026

Johnnidis, J.B., M.H. Harris, R.T. Wheeler, S. Stehling-Sun, M.H. Lam, O. Kirak, T.R. Brummelkamp, M.D. Fleming, and F.D. Camargo. 2008. Regulation of progenitor cell proliferation and granulocyte function by microRNA-223. *Nature.* 451:1125–1129. http://dx.doi.org/10.1038/nature06607

Karmakar, M., M. Katsnelson, H.A. Malak, N.G. Greene, S.J. Howell, A.G. Hise, A. Camilli, A. Kadioglu, G.R. Dubyak, and E. Pearlman. 2015. Neutrophil IL-1β processing induced by pneumolysin is mediated

Downloaded from http://rupress.org/jem/article-pdf/214/6/1737/1757972/jem_20160462.pdf by guest on 15 March 2025

by the NLRP3/ASC inflammasome and caspase-1 activation and is dependent on K^+ efflux. *J. Immunol.* 194:1763–1775. http://dx.doi.org/10.4049/jimmunol.1401624

Li, T., M.J. Morgan, S. Choksi, Y. Zhang, Y.S. Kim, and Z.G. Liu. 2010. MicroRNAs modulate the noncanonical transcription factor NF-κB pathway by regulating expression of the kinase IKKα during macrophage differentiation. *Nat. Immunol.* 11:799–805. http://dx.doi.org/10.1038/ni.1918

Ligumsky, M., P.L. Simon, F. Karmeli, and D. Rachmilewitz. 1990. Role of interleukin 1 in inflammatory bowel disease: Enhanced production during active disease. *Gut.* 31:686–689. http://dx.doi.org/10.1136/gut.31.6.686

Lopetuso, L.R., S. Chowdhry, and T.T. Pizarro. 2013. Opposing functions of classic and novel IL-1 family members in gut health and disease. *Front. Immunol.* 4:181. http://dx.doi.org/10.3389/fimmu.2013.00181

Mankan, A.K., T. Dau, D. Jenne, and V. Hornung. 2012. The NLRP3/ASC/caspase-1 axis regulates IL-1β processing in neutrophils. *Eur. J. Immunol.* 42:710–715. http://dx.doi.org/10.1002/eji.201141921

McNamee, E.N., J.D. Wermers, J.C. Masterson, C.B. Collins, M.D. Lebsack, S. Fillon, Z.D. Robinson, J. Grenawalt, J.J. Lee, P. Jedlicka, et al. 2010. Novel model of TH2-polarized chronic ileitis: the SAMP1 mouse. *Inflamm. Bowel Dis.* 16:743–752. http://dx.doi.org/10.1002/ibd.21148

McNamee, E.N., J.C. Masterson, P. Jedlicka, M. McManus, A. Grenz, C.B. Collins, M.F. Nold, C. Nold-Petry, P. Bufler, C.A. Dinarello, and J. Rivera-Nieves. 2011. Interleukin 37 expression protects mice from colitis. *Proc. Natl. Acad. Sci. USA.* 108:16711–16716. http://dx.doi.org/10.1073/pnas.1111982108

Mosser, D.M., and X. Zhang. 2008. Activation of murine macrophages. *Curr. Protoc. Immunol.* Chapter 14:Unit 14.2. http://dx.doi.org/10.1002/0471142735.im1402s83

Nagler-Anderson, C. 2001. Man the barrier! Strategic defences in the intestinal mucosa. *Nat. Rev. Immunol.* 1:59–67. http://dx.doi.org/10.1038/35095573

Nowarski, R., R. Jackson, N. Gagliani, M.R. de Zoete, N.W. Palm, W. Bailis, J.S. Low, C.C. Harman, M. Graham, E. Elinav, and R.A. Flavell. 2015. Epithelial IL-18 equilibrium controls barrier function in colitis. *Cell.* 163:1444–1456. http://dx.doi.org/10.1016/j.cell.2015.10.072

O'Connell, R.M., D.S. Rao, A.A. Chaudhuri, and D. Baltimore. 2010. Physiological and pathological roles for microRNAs in the immune system. *Nat. Rev. Immunol.* 10:111–122. http://dx.doi.org/10.1038/nri2708

Polytarchou, C., A. Oikonomopoulos, S. Mahurkar, A. Touroutoglou, G. Koukos, D.W. Hommes, and D. Iliopoulos. 2015. Assessment of circulating microRNAs for the diagnosis and disease activity evaluation in patients with ulcerative colitis by using the nanostring technology. *Inflamm. Bowel Dis.* 21:2533–2539. http://dx.doi.org/10.1097/MIB.0000000000000547

Pulikkan, J.A., V. Dengler, P.S. Peramangalam, A.A. Peer Zada, C. Müller-Tidow, S.K. Bohlander, D.G. Tenen, and G. Behre. 2010. Cell-cycle regulator E2F1 and microRNA-223 comprise an autoregulatory negative feedback loop in acute myeloid leukemia. *Blood.* 115:1768–1778. http://dx.doi.org/10.1182/blood-2009-08-240101

Ramkissoon, S.H., L.A. Mainwaring, Y. Ogasawara, K. Keyvanfar, J.P. McCoy Jr., E.M. Sloand, S. Kajigaya, and N.S. Young. 2006. Hematopoietic-specific microRNA expression in human cells. *Leuk. Res.* 30:643–647. http://dx.doi.org/10.1016/j.leukres.2005.09.001

Reinecker, H.C., M. Steffen, T. Witthoeft, I. Pflueger, S. Schreiber, R.P. MacDermott, and A. Raedler. 1993. Enhanced secretion of tumour necrosis factor-alpha, IL-6, and IL-1β by isolated lamina propria mononuclear cells from patients with ulcerative colitis and Crohn's disease. *Clin. Exp. Immunol.* 94:174–181. http://dx.doi.org/10.1111/j.1365-2249.1993.tb05997.x

Satsangi, J., M.S. Silverberg, S. Vermeire, and J.F. Colombel. 2006. The Montreal classification of inflammatory bowel disease: Controversies, consensus, and implications. *Gut.* 55:749–753. http://dx.doi.org/10.1136/gut.2005.082909

Schaefer, J.S., D. Montufar-Solis, N. Vigneswaran, and J.R. Klein. 2011. Selective upregulation of microRNA expression in peripheral blood leukocytes in IL-$10^{-/-}$ mice precedes expression in the colon. *J. Immunol.* 187:5834–5841. http://dx.doi.org/10.4049/jimmunol.1100922

Seo, S.U., N. Kamada, R. Muñoz-Planillo, Y.G. Kim, D. Kim, Y. Koizumi, M. Hasegawa, S.D. Himpsl, H.P. Browne, T.D. Lawley, et al. 2015. Distinct commensals induce interleukin-1β via NLRP3 inflammasome in inflammatory monocytes to promote intestinal inflammation in response to injury. *Immunity.* 42:744–755. http://dx.doi.org/10.1016/j.immuni.2015.03.004

Shouval, D.S., A. Biswas, Y.H. Kang, A.E. Griffith, L. Konnikova, I.D. Mascanfroni, N.S. Redhu, S.M. Frei, M. Field, A.L. Doty, et al. 2016. Interleukin 1β mediates intestinal inflammation in mice and patients with interleukin 10 receptor deficiency. *Gastroenterology.* 151:1100–1104. http://dx.doi.org/10.1053/j.gastro.2016.08.055

Song-Zhao, G.X., N. Srinivasan, J. Pott, D. Baban, G. Frankel, and K.J. Maloy. 2014. Nlrp3 activation in the intestinal epithelium protects against a mucosal pathogen. *Mucosal Immunol.* 7:763–774. http://dx.doi.org/10.1038/mi.2013.94

Zaki, M.H., K.L. Boyd, P. Vogel, M.B. Kastan, M. Lamkanfi, and T.D. Kanneganti. 2010. The NLRP3 inflammasome protects against loss of epithelial integrity and mortality during experimental colitis. *Immunity.* 32:379–391. http://dx.doi.org/10.1016/j.immuni.2010.03.003

Zaki, M.H., M. Lamkanfi, and T.D. Kanneganti. 2011. The Nlrp3 inflammasome: Contributions to intestinal homeostasis. *Trends Immunol.* 32:171–179. http://dx.doi.org/10.1016/j.it.2011.02.002

Zhang, J., S. Fu, S. Sun, Z. Li, and B. Guo. 2014. Inflammasome activation has an important role in the development of spontaneous colitis. *Mucosal Immunol.* 7:1139–1150. http://dx.doi.org/10.1038/mi.2014.1

Zhou, H., J. Xiao, N. Wu, C. Liu, J. Xu, F. Liu, and L. Wu. 2015. MicroRNA-223 regulates the differentiation and function of intestinal dendritic cells and macrophages by targeting C/EBPβ. *Cell Reports.* 13:1149–1160. http://dx.doi.org/10.1016/j.celrep.2015.09.073

Zigmond, E., C. Varol, J. Farache, E. Elmaliah, A.T. Satpathy, G. Friedlander, M. Mack, N. Shpigel, I.G. Boneca, K.M. Murphy, et al. 2012. Ly6C hi monocytes in the inflamed colon give rise to proinflammatory effector cells and migratory antigen-presenting cells. *Immunity.* 37:1076–1090. http://dx.doi.org/10.1016/j.immuni.2012.08.026

Downloaded from http://rupress.org/jem/article-pdf/214/6/1737/1757972/jem_20160462.pdf by guest on 15 March 2025